CoA NOTE MAT. No. 17

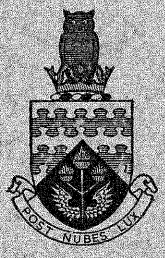

THE COLLEGE OF AERONAUTICS
CRANFIELD

A STUDY OF THE STRESS DISTRIBUTIONS NECESSARY TO MAINTAIN RUBBER IN A STATE OF TORSION

by

M. M. Hall

CoA Note Mat. No. 17

June, 1968

THE COLLEGE OF AERONAUTICS

DEPARTMENT OF MATERIALS

A study of the stress distributions necessary to maintain rubber in a state of torsion

- by -

M.M. Hall, B.Sc., Ph.D., A.Inst.P.

SUMMARY

Quantitative measurements have been made of the time dependent normal stress distributions and torques which are necessary to maintain a state of torsion in:

(i) a solid right circular cylinder of rubber,

(ii) rubber contained between a cone and touching flat plate.

The measurements on the solid rubber cylinder, under quasi-elastic conditions cannot be described by the kinetic theory of elasticity. There are considerable experimental difficulties involved in measurements on the cone and plate system but these results also suggest an inadequacy in the ability of the kinetic theory to describe finite deformations in rubbers.

Contents

List of symbols

W	stored elastic energy per unit volume
A, A', A_{pq}, B, B_{pq}, C, C_1, C_2, D, G, k_1, k_2, W_1, W_2, α, β	material parameters
I_1, I_2, I_3, J_1, J_2	strain invariants
λ	extension or compression ratio
t_{zz}, t'_{zz}	stresses normal to the plane ends of a cylinder
t_{oz}	tangential shear stresses
M	torque
F	force
σ_{ij}	stress tensor
σ	isotropic pressure
δ_{ij}	unit matrix
x_1, x_2, x_3	rectangular cartesian coordinates
r, θ, ϕ	spherical polar coordinates
h_1, h_2, h_3	defined by equation A.6
S_{ij}	strain tensor, defined by equation A.4
ψ	angle of twist per unit length, of a right circular cylinder
r, a	radii
$\frac{\pi}{2} - \beta$	semi-vertical angle of cone
η	angle of twist of cone
s	β/η
t	current time
t'	past time
Ω	a function of J_1, J_2 and $t-t'$

M_c	average molecular weight of rubber network chain
N	number of network chains per unit volume
m	mass
ρ	density
δQ	heat build up
J	mechanical equivalent of heat
k	Boltzmanns constants
T	absolute temperature

1. Introduction

There are a large number of commercial materials which may be classified under the general title 'rubbers'. Their common characteristic is the ability to support finite reversible strains. The elastic properties of these materials are completely defined if the energy stored during an isothermal elastic deformation can be described by an analytical function.

A previous Note (Hall, 1968) reviewed the various empirical forms of the stored energy function W which have been proposed. In each case W was a function of the strain invariants I_1 and I_2. This was seen to be at variance with the kinetic theory of elasticity which predicts that, within certain strain limits, W is a function of I_1 only. Stress relaxation measurements upon sheet rubber in a state of pure homogeneous deformation suggested that $\partial W/\partial I_2$ was finite and the kinetic theory therefore inadequate to describe this deformation.

A complete characterisation of the stored energy function involves the description of the surface W (I_1,I_2) when W, I_1 and I_2 are mutually orthogonal co-ordinate axes. The measurements on sheet rubber involved an examination of the surface over a particular set of contour lines. These are defined by the relationships between I_1 and I_2 which are imposed by the pure homogeneous deformations examined.

This Note describes measurements of the stress system needed to maintain a solid cylinder of rubber in a state of torsion. The distribution of the stresses in a torsion system has a particularly direct relationship to $\partial W/\partial I_2$ and other material parameters of the stored energy function along the contour line $I_1 = I_2$ of the surface W (I_1,I_2). It therefore allows a further and critical examination of the theories of rubberlike elasticity.

The stress distributions necessary to maintain a state of torsion in rubber which is bonded between a cone and touching flat plate has also been considered.

2. The torsion of rubber

2.1 Torsion of a right circular cylinder

It has been shown by Rivlin (1948a, 1948b, 1956) that the surface tractions necessary to maintain a right circular solid cylinder in a state of torsion correspond to two sets of stress components, each acting only over the plane ends of the cylinder. In addition to the distribution of tangential surface tractions providing the twisting couple, a distribution of normal surface tractions is required to maintain the cylinder at constant length.

Let the cylinder be twisted so that each section perpendicular to the axis rotates through an angle proportional to its distance from one end of the cylinder. Then according to Rivlin

$$I_1 = I_2 = 3 + \psi^2 r^2, \quad I_3 = 1 \tag{2.1}$$

Since $I_3 = 1$ there is no volume change on deformation, and the complete stress system can be expressed in terms of the derivatives of the stored energy function W with respect to I_1 and I_2. The normal stress t_{zz} at a distance r from the axis of the cylinder of radius a, and the torsional couple M, are given by,

$$t_{zz} = 2\psi^2 \int_a^r r \frac{\partial W}{\partial I_1} dr - 2\psi^2 r^2 \frac{\partial W}{\partial I_2} \tag{2.2}$$

and

$$M = 4\pi\psi \int_0^a r^3 \left(\frac{\partial W}{\partial I_1} + \frac{\partial W}{\partial I_2} \right) dr \tag{2.3}$$

where ψ is the angle of twist per unit length.

It can be seen that if the form of W is known then the stress system is uniquely determined.

From (2.2) the normal stress on the axis of the cylinder is given by

$$\left(t_{zz} \right)_{r=o} = 2\psi^2 \int_a^o r \frac{\partial W}{\partial I_1} dr \tag{2.4}$$

and therefore depends only on the material parameter $\frac{\partial W}{\partial I_1}$. The normal stress at the edge of the cylinder depends only on $\frac{\partial W}{\partial I_2}$, and is given by,

$$\left(t_{zz} \right)_{r=a} = - 2\psi^2 a^2 \frac{\partial W}{\partial I_2} \tag{2.5}$$

The kinetic theory of elasticity expresses W in terms of I_1 only, and then $\frac{\partial W}{\partial I_2} = 0$. Hence if under equilibrium conditions the normal stress at the edge can be shown to be finite, then the kinetic theory will have been shown to be inadequate to characterise this deformation.

From the kinetic theory $W = C_1 (I_1 - 3)$ and substitution into (2.2) and (2.3) gives

$$t_{zz} = \psi^2 (r^2 - a^2) C_1 \tag{2.6}$$

and

$$M = \pi\psi a^4 C_1 \tag{2.7}$$

and hence

$$\left(t_{zz}\right)_{r=o} = -\psi^2 a^2 C_1 \qquad (2.8)$$

and

$$\left(t_{zz}\right)_{r=a} = 0$$

If the Mooney form of the stored energy function is correct, $W = C_1(I_1-3) + C_2(I_2-3)$, (Mooney 1940, 1964) and then

$$t_{zz} = -\psi^2\left[C_1(a^2-r^2) + 2r^2C_2\right] \qquad (2.9)$$

and

$$M = \pi\psi a^4(C_1+C_2) \qquad (2.10)$$

and hence $$\left(t_{zz}\right)_{r=o} = -\psi^2 a^2 C_1 \qquad (2.11)$$

and $$\left(t_{zz}\right)_{r=a} = -2\psi^2 a^2 C_2 \qquad (2.12)$$

The total normal force acting over the end plate is given by

$$N = \int_o^a 2\pi r\, t_{zz}\, dr \qquad (2.13)$$

For the Mooney function,

$$N = -\tfrac{1}{2}\pi\psi^2 a^2(C_1+2C_2) \qquad (2.14)$$

2.2 Torsion of a cone and plate sample

Suppose the rubber is bonded between a cone of semi-vertical angle $\frac{\pi}{2} - \eta$, and a touching flat plate which is perpendicular to the cone axis. Let the rubber be deformed by twisting one end plate with respect to the other in a plane perpendicular to the sample axis. Equations have been developed (Appendix 1) to describe the two sets of surface tractions which must be applied over the end plate in order to maintain the sample in a state of torsion, and the cone and plate in contact.

If the composite specimen forms a cylinder of radius a, then the torque M required to twist the sample through an angle β is given by

$$M = \frac{4}{3}\pi a^3 s \left(\frac{\partial W}{\partial I_1} + \frac{\partial W}{\partial I_2}\right) \tag{2.15}$$

where $s = \beta/\eta$. Furthermore t_{zz}, the normal stress at a distance r from the sample axis, measured in the plane of the flat plate, is given by

$$t_{zz} = -2s^2 \left(\frac{\partial W}{\partial I_1} - \frac{\partial W}{\partial I_2}\right) \ell n \frac{a}{r} - 2s^2 \frac{\partial W}{\partial I_2} \tag{2.16}$$

hence

$$\left(t_{zz}\right)_{r=a} = -2s^2 \frac{\partial W}{\partial I_2} \tag{2.17}$$

These equations are only accurate if the boundary of the rubber is a sphere centred on the cone apex. However the errors are small when the boundary is cylindrical if η is small.

The linear relationship between t_{zz}, and $\ell n \frac{a}{r}$ predicted by (2.16) should be maintained for any analytical form of the stored energy function $W(I_1,I_2)$ (Appendix 1). The graphical determination of the complete normal stress distribution, from a limited number of experimental points, is therefore, in principle, much easier for a cone and plate system than a parallel plate system.

3. Torsion equipment

The apparatus was designed to twist the lower plane surface of the parallel plate cylindrical sample relative to the top surface. Whilst accurately maintaining the sample at its undeformed length. Equipment has also been developed to measure the force system involved in the torsion.

3.1 General details of the torsion jig and sample

The apparatus which has been developed is shown diagrammatically in Figure 1. The sample S, in the form of a solid rubber cylinder of about 10 cms. in diameter and 1.5 cms. in length, is bonded during vulcanisation to two mild steel end plates. This composite sample is mounted on a platform P and held in position by a diametric key, and a matching keyway in the bottom end plate C. The end plate B is rigidly fastened to A, the top plate of the jig, which in turn is fastened to the main body of the apparatus. The internal separation between the top plate of the jig and the platform is equal to the length of the undeformed composite sample.

The platform forms an integral unit with a torque tube T which is supported by a set of taper roller bearings E, and alignment of the sample and torque tube axes is maintained by a ball race bearing D. The torque to the sample is applied by hand via the torque tube and the worm and wheel

gearbox G. This gearbox has a ratio of 225/1 and incorporates a locking device to hold the sample in any desired state of torsional deformation. Calibration has established that the movement of the drive to the gearbox may be used as an accurate indicator of the movement of the bottom plate.

Five 1 cm. diameter holes are cut through the top plate of the sample and torsion jig. During torsion the rubber, if it was unrestrained, would bulge into these holes. In practice restraints are applied to prevent bulging, and the necessary normal forces are measured.

3.2 Design problems of the jig and sample

In designing the equipment the initial problems were concerned with deciding upon the overall sample dimensions. The magnitude of the forces involved in applying the required deformations could then be estimated, and the torsion jig designed. Considerable attention was given to minimizing sources of error that affect measurement of the applied stress system.

3.2.1 The sample

The limiting factor governing the overall diameter of the sample was the size of the torque necessary to produce finite shear strains. Preliminary experiments had shown that a bond could be formed between a rubber cylinder and metal end plates which would withstand shear strains of 100% at the curved surface of the sample. The equipment was designed to be capable of applying a surface shear strain of 200%. At this strain level occasional bond failure was observed, and on one occasion failure occurred in the rubber itself. The maximum torque required to produce a surface shear strain of 200% was estimated using 2.10. The value of C_1 and C_2 were the maximum values of $\frac{\partial W}{\partial I_1}$ and $\frac{\partial W}{\partial I_2}$ determined by simple elongation measurements on a number of crosslinked gum rubbers. (Appendix 2.2). The calculations showed that a torque of about 3,500 kg.cms. would be needed to apply the required deformation to a sample of 5 cms. radius. This was considered to be a reasonable upper limit to the torque requirement in order to minimize difficulties in designing the torsion jig.

The forces normal to the plane ends of the sample were to be determined by restraining the rubber from bulging into the five circular holes disposed over the top metal end plate. In choosing a suitable hole size account was taken of two opposing requirements. The forces to be measured, and hence the sensitivity of measurement increased with increasing hole diameter. However, large hole diameters necessarily involve large sample diameters since there are three requirements that the hole to sample ratio should be kept small. These are:-

1. The necessity to reduce interference between the holes.

2. The requirement that the average normal stress over the free rubber surface should be equal to the normal stress at the position occupied by the centre of the hole.

3. The tangential stresses required in torsion are not applied over the free rubber surface in the hole, which leads to a local variation in the state of pure torsion, and must be minimized.

A preliminary experiment was carried out to estimate the degree of unrestricted bulging into the holes that would be caused by the normal stresses. A natural rubber sample with bonded metal end plates was twisted by hand using a crowbar inserted into the lower plate.

The sample was held by a rigid frame so that expansion under the action of the normal forces was prevented. The rubber was allowed to bulge into two holes on the same diameter of the top plate, and equidistant from the sample axis. The hole diameters were 1.27 cms. and 0.95 cms. and the bulge heights were measured using a dial gauge which registered the displacement of a plunger resting on the free rubber surface. A counter balance system was used to overcome the inertia of the plunger, and hence prevent errors in measurement due to indentation of the plunger into the rubber. Extrapolation of the experimentally determined linear relationship between bulge height and ψ^2 suggested that for a 200% surface shear strain the rubber would bulge about 0.1 cms. into the 0.95 cms. diameter hole.

The optimum distribution of holes in the end plate was not determined until the torsion jig had been built. Then the normal stress interference was studied by measuring the unrestrained bulge heights for various arrangements of holes. The torsion was maintained constant and selected holes in the top plate were closed by accurately machined plugs. The effect of closing one or more holes upon the measured bulges in the remaining free holes was examined. With the hole size and arrangement chosen no interference was detected. At least five holes at different radial distances from the sample axis were considered to be necessary to determine the normal stress distribution.

The errors involved in assuming that the average normal stress over the free rubber surface in a hole is equal to the normal stress at the centre of that hole have been estimated (Appendix 3).

The sample length was chosen to be about 1.5 cms. If the samples are too long then visual examination revealed an inhomogeneous state of cure because of the inadequate rate of heat conduction into the rubber during vulcanisation.

Calculations have been carried out on the effects of the temperature rise to be expected on deformation of the rubber. A large proportion of the free energy of deformation is due to entropy changes, and, therefore, deformation is accompanied by a heat interchange between the rubber and surroundings. Calculations showed (Appendix 4) that these temperature changes are unlikely to have a significant effect upon normal stress and torque measurements.

The rubbers were valcanised at 150°C. Details of the preparation of the samples, and the recipes of the rubbers, are given in Appendix 2.1. In cooling the samples to room temperature there must be internal stresses

set up in the rubber due to the differential thermal contractions of the bonded rubber and metal end plates. Torsion and compression experiments were carried out on rubber which was bonded during vulcanisation at 150°C, and on similar rubbers bonded to the end plates using a room temperature curing adhesive (Eastman 910). The force systems measured for the two types of deformations were independent of the method of bonding. The effect of the internal stresses can therefore be ignored.

The bonds formed at room temperature between the end plates and rubber vulcanised with dicumyl peroxide were not able to support the shear strains involved in torsion, and hence all samples were bonded during vulcanisation.

The torsion jig was also used to twist cone and plate samples. They were of the same overall length as the parallel plate samples but with a different distribution of holes over the flat end plate. It was necessary to bond the rubber to the end plates at room temperature, otherwise the differential thermal contractions would set up strains in the rubber comparable to the applied torsional strains.

The details of the parallel plate, and cone and plate samples are given in figure 2.

3.2.2 The torsion jig

The equipment must be rigid enough to stop the sample extending under the maximum total normal force exerted by this sample. The torsion data of Rivlin and Saunders (1951), obtained on a rubber similar to rubber No. 3, suggests that the total normal force exerted by a parallel plate sample with the dimensions shown in figure 2 will be about 100 kg. at 100% surface shear strain.

The major source of axial movement is in the bearings. The sample is completely supported by preloaded taper roller bearings which allow a movement of 5.10^{-4} cms. under a 100 kg. load (Manufacturers data). The dimensions of the top plate of the torsion jig, and the sample platform and torque tube, are such that the total flexure allowed by these units under the load is about 10^{-4} cms. The total vertical movement under a 100 kg. load is therefore limited to 6.10^{-4} cms.

In assembling the jig careful alignment ensured that the platform remained parallel to the top plate of the jig during rotation. The distance between the top plate and platform remained constant to an accuracy between than 10^{-4} cms. The normal forces measured as a function of the torsional strain, were later found to be independent of the direction of rotation of the platform, demonstrating the uniformity of motion of the platform under pressure (Section 4.2.1).

Measurements will underestimate the magnitude of the normal stress because of the axial movement. The error at 100% surface shear strain can be considered to be the stress needed to compress the 1.51 cm. long sample by

6.10^{-4} cms, to restore it to its undeformed length. For this very small strain it is adequate to calculate the compressive stress from Hookes law. It is simple to show, that the initial Youngs modulus for a rubber described by the Mooney stored energy function is $6(C_1+C_2)$. Now for a typical natural rubber gum $(C_1+C_2) = 2$ kg. cm.$^{-2}$ (Rivlin and Saunders, 1951). The compressive stress is then about 5 g.cm^{-2}. An error of 5 g.cm^{-2} at all radial distances over the end plate, for a surface shear strain of 100%, ($\Psi a = 1$), is equivalent to an error of 5 g.cm^{-2} in C_1, and 2.5 g.cm^{-2} in C_2 (using (2.11) and (2.12)). The values of C_1 and C_2 determined by simple extension measurements are of the order of 10^3 g.cm^{-2} and 10^2 g.cm^{-2} respectively. (For example, Ciferri and Flory, 1959). The relative errors in C_1 and C_2 due to axial movement, will therefore be small.

3.3 The force measuring equipment

It was necessary to design equipment which would determine the magnitude of the forces needed to restrain bulging in the holes of the end plate when the sample was twisted.

The maximum normal stress, for a given strain, acts on the axis of the sample and is given by (2.11). The corresponding force acting over the area of an 0.95 cm. diameter hole is about 7 kg. for a well vulcanised rubber with a 200% surface shear strain. (Typically $C_1 \sim 2.5$ kg.cm^{-2} Appendix 2.2). The torsional couples to be measured are less than 3500 kg.cms.

3.3.1 The normal load dynamometers

A dynamometer assembly has been developed to measure the normal forces (Figure 3).

The lightweight ('perspex') plunger A rests on the free rubber surface. Vertical movement of A are transmitted through the ball B to the yoke C, which is supported from the tube D by six thin wires. The wires are in tension and prevent lateral movement of the yoke. Vertical movements were limited to less than 10^{-4} cms., and are virtually frictionless over this range.

A sensitive and stable position indicator, in the form of a Sogenique concentric cylinder capacity transducer, is used to indicate the position of the yoke C relative to the tube D.

The dynamometer is set up so that the position indicator reads zero with the plunger A just resting on the free rubber surface at zero torsion. Torsion of the cylinder then causes vertical movement of A, which is detected by the transducer and reduced to zero by screwing down the micrometer head F compressing the calibrated spring E against the yoke C. The forces applied to C may then be obtained from the micrometer head reading. This force, divided by the effective cross-sectional area of the dynamometer plunger, is taken to be the value of the normal stress at the centre of that free surface. The error involved in that assumption is estimated in Appendix 3.

During the development stage an alternative system for the measurement of normal stresses was investigated. This consisted of restraining the rubber bulges by a rigid plunger of transparent resin. The stresses were then to be determined by photoelastic examination of the resin. Although in principle it had advantages over the dynamometer system described, calculations showed that it was not readily capable of yielding such a high sensitivity. (Appendix 5).

3.3.2 The Torque tube

The torque required to deform the rubber sample may be measured by determining the deformation of a high tensile steel torque tube. Four resistance strain gauges are fixed to the tube surface with an epoxy resin adhesive, and are arranged in a Wheatstones Bridge network so that the balance of the bridge is affected only by torsional deformation.

Friction in the ball race bearing is negligible compared with the torque required to deform the rubber sample, and friction in the thrust bearing does not affect the deformation of the torque tube.

3.4 Calibration of the force measuring equipment

3.4.1 The normal load dynamometers

A chemical balance was modified so that a known load could be applied to the dynamometer. The arrangement is shown in figure 4a.

A rod J was fastened above one arm of the balance, and counterbalanced by weights added to the pan on the opposite arm. The dynamometer was mounted rigidly above the balance so that the rod J just made contact with the ball B. Known loads were applied to B, and hence the yoke C, by the addition of weights to the appropriate pan. The yoke was maintained in its original position by compression of the spring E with the micrometer head F, the position being detected by the null deflection method using the transducer head reading against the load acting on the dynamometer at A is shown in figure 4b.

No hysteresis was observed in loading and unloading the dynamometers during calibration as long as sudden changes in the forces on the yoke were kept below 10 grams.

The dynamometers were sensitive to load changes of less than 1 gram at all points on the calibration curve.

3.4.2 The effective area of the dynamometer plunger

A dynamometer measures the compressive force needed to maintain the plunger A at the level of the undeformed free rubber surface. When this compressive force is in equilibrium with the normal force in the rubber, then some bulging of the rubber must still occur over the free annular surface

between the plunger and the edge of the hole. Hence to calculate the normal stress on the axis of the plunger, for a known normal load, it is necessary to know the effective area of the plunger.

A pure compression experiment was carried out on a natural rubber gum-stock sample of the same dimensions as the torsion samples. Known compressive stresses t were applied and the forces F needed to restrain bulging in the centre hole of the top plate were measured (Figure 4c). The effective area of the plunger, S, is defined as the ratio of F to t, and hence $S = 0.51 \pm 0.01$ cm^2. The actual plunger area was 0.495 cm^2, and the hole area 0.71 cm^2. Tn ensure pure compression the end surfaces of the rubber sample were lubricated with silicone fluid, and the compressive strain was limited to about 1%.

3.4.3 The torque tube

The deformation of the torque tube was calibrated by noting the current output for the strain gauge network, using a Phillips A.C. Bridge, type PT1200/01, when known torques were applied to the tube. The torque tube was twisted in both directions and both calibration curves are linear (figure 4d).

The difference in gradient of the two curves is the result of a small asymmetry in the arrangement of the four strain gauges with respect to the torque tube axis. There was no hysteresis in the deformation. Thrust loads several times larger than those experienced during the experiments had no effect upon the calibration.

4. Torsion Procedure and Results

4.1 Experimental procedure

The sample was mounted on the platform of the torsion jig and clamped to the top plate, which in turn was rigidly fastened to the main body of the jig.

Metal shims were inserted into the space between the top plate and the main body in an attempt to hold the sample at its undeformed length. There are considerable difficulties in ensuring that the sample fits accurately into the gap between the top plate and the supporting platform. If the gap is too large then the dynamometers will not record a normal load until the rubber has extended under torsion to fill the gap. In practice the shims were such that the sample was maintained in a state of strain corresponding to an axial compression of 5.10^{-4} cms. or a compression ratio $\lambda = 0.9998$ for a 1.51 cm. sample. This compression was determined by measuring the unrestricted bulge height in the centre hole of the sample end plate. Preliminary experiments had shown that an axial compression of 5.10^{-4} cms. corresponded to a bulge height of about 10^{-3} cms.

The effect of an axial compression superimposed on the torsion of a cylinder has been considered by Rivlin (1949a). If the rubber is

characterised by the Mooney stored energy function then the normal stress t_{zz} and the total torque M are given by

$$t_{zz} = 2\left(\lambda^2 - \frac{1}{\lambda}\right)\left(C_1 + \frac{C_2}{\lambda}\right) + \psi^2\left[\lambda C_1(r^2-a^2) - 2r^2C_2\right] \qquad (4.1)$$

$$M = \pi\psi a^4\left(C_1 + \frac{C_2}{\lambda}\right) \qquad (4.2)$$

The first term in (4.1) is independent of ψ, and will not affect normal stress measurements because the dynamometer uses the position at $\psi = 0$ of the free rubber surface in the holes as the reference position. The effect of a compression $\lambda = 0.9998$ upon t_{zz} and M can be seen from (4.1) and (4.2) to be negligible.

4.1.1 Elastic Rubbers

The surface tractions applied to the parallel plate, and cone and plate systems were measured for rubbers which exhibited very little time dependence in their mechanical properties (rubber nos. 1 to 5).

Equal increments of torsional strain were imposed and after a fixed time at each strain the normal force at each hole and the total applied torque was measured. The complete strain cycle was examined with 2 minute time intervals between the strain increment and load measurements, and then repeated with 10 minute time intervals. At least 24 hours was allowed between cycles for the relaxation of residual stresses. The residual torque became zero less than 4 hours after ψ was returned to zero. Care was taken to ensure that there were no sudden changes in the force on the dynamometers, and therefore, no hysteresis exhibited by them. In any one strain cycle the size of the dynamometers did not allow the forces at all the holes to be measured. Two cycles for each sample were necessary for measurements at the 5 holes.

For each parallel plate natural rubber sample the unrestrained bulge height into the centre hole was determined as a function of the torsional strain.

Ambient temperatures were noted.

4.1.2 Time dependent rubbers

In order to examine stress relaxation effects parallel plate samples were made from a fully crosslinked butyl rubber (rubber No. 7) and a lightly crosslinked natural rubber (rubber No. 6).

The butyl rubber exhibits stress relaxation at 0°C because of the broad energy loss peak associated with its glass transition temperature. An enclosure was built around the torsion jig and filled with melting ice in an

attempt to allow measurement at 0°C. Unfortunately dimensional instability in each dynamometer, because of non-equilibrium temperatures, resulted in a variable output from the sensitive displacement transducers which made it impossible to discriminate variations due to stress relaxation.

Electrical heaters incorporated in the enclosure allowed the butyl rubber to be further examined at 25°C. At this temperature no stress relaxation was observed.

The natural rubber No. 6 was examined at 19°C. A surface shear strain of 132% was applied in 30 seconds, at a constant strain rate. This deformation was then maintained constant. The normal forces and torque were determined at intervals over a period of time. In order to measure the normal forces at each of the 5 holes in the end plate it was necessary to examine two samples because of the size of the dynamometers The same sample could not be used twice because of the unknown effect of the strain history. Each sample was prepared from the same rubber mix, and moulded under identical conditions.

4.2 Experimental results

4.2.1 Elastic Rubbers in the parallel plate system

The complete results are given in Tables 1 and 2.

Sample No. 1 was twisted in both directions to check the uniformity of the torsion jig. The arithmetic mean and range of the normal loads are quoted. At any one hole the normal load for a particular direction of twist was consistently greater than, or equal to, the loads measured on twisting in the opposite direction. However the correlation of greatest load with a particular twist suggest uniformity in the jig and indicate the degree of reproducibility that can be attained.

There are no systematic deviations from linearity in the relationships between the normal stress at a point and ψ^2 (Figures 5 to 10), but the variation of torque with ψ exhibits the characteristic non-linearity reported earlier by Rivlin and Saunders (1951). (Figures 11 to 13). For clarity only the results obtained as the strain was increased are shown. There are residual strains in the sample when ψ is returned to zero. These strains become zero in a time about equal to the time taken for a complete deformation cycle.

The normal stress distributions for surface shear strains of 130% are shown in Figures 14 and 15.

The normal stress at the edge of the sample depends only on the derivative $\frac{\partial W}{\partial I_2}$ of the stored energy function. An attempt has been made to extrapolate the distributions to the edge of the sample. If the rubbers can each be characterised by a stored energy function of the same analytical form, then

the distributions for each rubber will also have the same form. Examination of figures 16 and 17 suggest that at distances greater than about 3 cms. from the sample axis only a linear distribution can give a reasonable fit for all rubbers. This is supported by the distributions obtained at 100% surface shear strain using normal stress values taken from the decreasing strain part of the deformation cycle. (Figures 16 and 17).

Hysteresis for each cycle is estimated by considering the ratio of the area enclosed by the normal stress - ψ^2 loop to the area under the increasing strain curve (Table 3).

Rubber	Hysteresis (%) 2 minute time interval	10 minute time interval
No. 1 at 20°C	9	
No. 2 at 19°C	8	6
No. 3 at 19°C	15	15
No. 4 at 18°C	14	13
No. 5 at 20°C	17	14
No. 7 at 25°C		0

Table 3 Hysteresis estimated from the normal stress measurements

There is no regular variation of hysteresis with radial position, and the mean hysteresis for all five holes of each sample is slightly reduced when the time interval between a strain increment and stress measurement is increased from 2 minutes to 10 minutes.

The torque measurements for all rubbers exhibit a small amount of hysteresis. The variation of torque with ψ over the complete strain cycle, for rubber No. 7, is shown in Figure 13.

After carrying out measurements on rubbers 1 and 4 it was found necessary to reduce the maximum shear strain involved because a natural rubber cross-linked with 3% by weight of dicumyl peroxide fractured when twisted through 30°.

It can be seen from Figure 18 that there is a linear relationship between the normal stress and the unrestrained bulge height measured in the central hole of the end plate of each sample. This substantiates the conjecture of Rivlin (1947). Because all the holes are of the same size, the difference in the gradients of the straight lines is due only to the difference in the material properties of each sample. Furthermore, measurements made in all 5 holes in the end plate of rubber No. 1 show that the gradient is independent of radial position (Figure 19). All measurements were made at 2 minute intervals after the strain increment.

The natural rubber samples were examined at temperatures between 18°C and 20°C. The temperature varied by less than 1°C as measurements were made on any one sample.

4.2.2. Elastic rubbers in the cone and plate system

Rubber Nos. 1 and 7 were examined at 18°C. The loads were measured 10 minutes after each strain increment. The variation of normal stress with s^2, at different radial distances from the sample axis, is shown in Figures 20a and 20b. Considerable difficulty was experienced in obtaining a satisfactory bond between the rubber and the metal end plates at room temperature. Subsequent examination of the interface of the samples upon which measurements were made showed several small areas of poor adhesion. When these occurred in the vicinity of a hole through the end plate then normal force measurements in that hole were discarded. These difficulties may well account for the deviations from linearity, in arbitrary directions, of the normal stress vs.s^2 graphs.

The normal stress as a function of $\ell n\ a/r$, for $s = 0.8$ (expected from 4.16 to be a linear relationship) is shown in figure 21.

The variation of the torque with s, (Figure 22), shows a non-linearity of the type found for parallel plate samples.

Although the results obtained are of interest, the difficulties in sample preparation and the increased effect of the errors inherent in the torsion jig, completely offset the advantages of having a known analytical form for the normal stress distribution.

4.2.3 Time dependent rubbers

The relaxation of normal stress in each of the 5 holes in the end plate of rubber No. 6, is given in Table 4 and shown in Figure 23. The surface shear strain was maintained constant at 132%. Equilibrium stress values were not observed. Stress measurements in holes B, C, and E were made on one sample and measurements in A and D were made on another sample prepared in exactly the same way.

The variation of torque with time (table 4) is shown in Figure 24. No significance can be attached to the apparent approach to an equilibrium value because zone drift is more likely to have occurred in the bridge network which determined the magnitude of the torque. Previous observations had shown the drift to be as much as 5% of the total torque reading for times greater than 300 minutes. The torque measurements did not detect any difference in the mechanical properties of the two samples which were necessary to complete measurements on any one rubber.

5. Analysis of the torsion results

5.1 Elastic Rubbers

The first objective was to examine $\frac{\partial W}{\partial I_2}$. If $\frac{\partial W}{\partial I_2}$ is finite under equilibrium conditions then the Kinetic theory is inadequate to describe the experimental results.

Equation 2.2 states that the stress normal to the plane end surfaces of the cylinder, at any general position $0 < r < a$ is dependent upon the material parameters $\frac{\partial W}{\partial I_1}$ and $\frac{\partial W}{\partial I_2}$. $\frac{\partial W}{\partial I_2}$ can be determined from the normal stress at $r = a$, the edge of the sample, but there are difficulties in the extrapolation of a distribution of unknown form. The straight line extrapolations of the normal stress distributions shown in Figures 14 to 17 have been used to calculate the magnitude of $\frac{\partial W}{\partial I_2}$. If $\frac{\partial W}{\partial I_1}$ is independent of strain and denoted by the material constant A, then A can be calculated from the normal stress at $r = 0$. The value of A and $\frac{\partial W}{\partial I_2}$ for the different rubbers are given in Table 5.

The limited stress relaxation which occurs as the time between the strain increments and stress measurements is increased from 2 minutes to 10 minutes, is reflected in the small reduction in A. There is no corresponding systematic change in $\frac{\partial W}{\partial I_2}$. Furthermore, because there is a linear relationship between the normal stress t_{zz} and ψ^2 at all 5 holes, a straight line extrapolation of the distribution will necessarily give a value for $\frac{\partial W}{\partial I_2}$ which is independent of strain.

The observed linear relationship between t_{zz} and ψ^2 for decreasing strains lies below the increasing strain results In the limiting case when the surface tractions are reduced to zero there is still a finite strain and therefore A and $\frac{\partial W}{\partial I_2}$ determined from the increasing strain part of the cycle. The time dependence of the residual strain is reflected in the increase in $\frac{\partial W}{\partial I_2}$ as the time interval is increased to 10 minutes.

The values of $\frac{\partial W}{\partial I_2}$ in Table 5 are finite. The range of possible errors are indicative of the difficulties of extrapolation. It is important to notice that there is no reduction in $\frac{\partial W}{\partial I_2}$ as the time interval is increased to 10 minutes. Preliminary experiments had not detected further normal stress relaxation in time intervals up to 8 hours. It is reasonable to suppose therefore that these values for $\frac{\partial W}{\partial I_2}$ will not alter significantly under true equilibrium conditions.

A number of stored energy functions have been examined in an attempt to describe the experimental results. It has been seen (2.9) that the Mooney stored energy function predicts a parabolic relationship between t_{zz} and r, and a linear relationship between the torque M and ψ (2.10). The non-linearity between M and ψ immediately exposes the inadequacy of this function to describe the results completely. The Mooney parameters C_1 and C_2 have been determined by obtaining the best fit between (2.9) and the experimental results, which are presented in Figures 25 to 28 with t_{zz}/ψ^2 as the ordinate, and a^2-r^2 as the abscissa.

The straight line through each set of points was determined by the least squares method. According to (2.9) the gradient of each line is $(C_1 - C_2)$, and the intercept with the ordinate is $2a^2C_2$. The calculated values of C_1 and C_2 are given in Table 6.

The values of C_2 are less than the corresponding values of $\frac{\partial W}{\partial I_2}$ in Table 5. This is of course a consequence of the curvature of the parabolic distribution. Negative values of C_2 are obtained for rubber nos. 4 and 5. It is important to realise that, unlike $\frac{\partial W}{\partial I_2}$ in table 4, C_1 and C_2 are influenced by the normal stress measurement at all 5 holes in the end plate. Examination of Figures 25 to 28 shows that a positive C_2 would have been obtained for rubbers 4 and 5 if the normal stress on the axis had been ignored. This is equivalent to assuming that the normal stress measured at r = 0 for these rubbers is too high. However, figures 25 to 28 suggest that the experimental points for all the rubbers may best be described by curves which are slightly concave to the $a^2 - r^2$ axis. Then extrapolation to r = a would give a positive $\frac{\partial W}{\partial I_2}$ and the values of C_2 in table 6 are too low because of the inadequacy of the Mooney function. Furthermore C_2 increases as the time between stress measurements is increased to ten minutes. This is at variance with the behaviour of C_2 determined from simple extension measurements. (Ciferri and Flory 1959). The Mooney normal stress distributions are shown in Figure 29 for rubber at 130% surface shear strain, and compared with experimental points obtained from stress measurements at 10 minute intervals as the strain is increased.

For a Mooney rubber the gradient of the torque - ψ relationship is proportional to $C_1 + C_2$ (2.10). The non-linearity of the experimental results, Figures 11 to 13, suggest that $C_1 + C_2$ is strain dependent. The gradients at small strain, and at $\psi = 0.256$, $(\psi a = 1.3)$, have been measured and $C_1 + C_2$ evaluated. (Table 7). There is a considerable difference between $C_1 + C_2$ determined from the torque, and from normal stress measurements on the same rubber. This may be a further illustration of the inadequacy of the Mooney function, or a consequence of errors in the torque, or normal stress measurements. The equipment has been fully discussed in section 3. No source of errors of this magnitude is known.

The empirical stored energy function proposed by Gent and Thomas (1958) has been examined.

i.e. $$W = W_1 (I_1-3) + W_2 \ell n \frac{I_2}{3} \qquad (5.1)$$

where W_1 and W_2 are constants and related to the Mooney parameters so that

$$W_1 = C_1 + p C_2$$

$$W_2 = qC_2 \qquad (5.2)$$

The constants $p = 0.247$ and $q = 2.18$ were chosen by Gent and Thomas so that the predicted stress-strain relation in simple extension would give a good fit to experimental results over the range $1.15 < \lambda < 1.7$.

Substitution of (5.1) and (5.2) into the general expressions for the normal stress and torque ((2.2) and (2.3)) and evaluation of the integrals, gives

$$t_{zz} = (C_1+pC_2)\psi^2(r^2-a^2) - \frac{2qC_2\psi^2r^2}{\psi^2r^2+3} \qquad (5.3)$$

and

$$M = \pi\psi a^4(C_1+pC_2) + \frac{2\pi a^2qC_2}{\psi} - \frac{6\pi qC_2}{\psi^3} \ell n \frac{\psi^2a^2+3}{3} \qquad (5.4)$$

and therefore on the axis of the sample

$$\left(t_{zz}\right)_{r=o} = - (C_1+pC_2)\psi^2a^2 \qquad (5.5)$$

and at the edge of the sample

$$\left(t_{zz}\right)_{r=a} = - \frac{2qC_2\psi^2a^2}{\psi^2a^2+3} \qquad (5.6)$$

The normal stress function (5.3) is shown in figure 30, using the values of C_1 and C_2 in table 6. For positive values of C_2 the compressive normal stress on the axis is larger than the corresponding Mooney stress, since p is positive. The normal stress at the edge is less than the corresponding Mooney stress because $\psi^2a^2 + 3 > q$. The Gent-Thomas and Mooney normal stress distributions must therefore cross over at some radial distance from the axis which is dependent upon the strain. For small strains the difference between the two distributions will be negligible. This is not surprising because the logarithmic function in (5.1) can be expanded* so that

---

* The series expansion for $\ell n\,(1+x)$, for $-1 < x \leq 1$, is given by

$$\ell n(1+x) = x - \frac{x^2}{2} + \frac{x^3}{3} - \frac{x^4}{4} + \ldots.$$

If $1 + x = I_{2/3}$, then $x = (I_2 - 3)/3$ where $I_2 \leq 6$.

$$W = W_1(I_1-3) + \frac{W_2}{3}(I_2-3) - \frac{W_2}{18}(I_2-3)^2 + \ldots. \qquad (5.7)$$

provided that $I_2 \leq 6$. If the strain is small enough to neglect squares and higher powers of I_2-3 then (5.7) is a function of the Mooney form, $W = C_1(I_1-3) + C_2(I_2-3)$.

The onset of non-linearity in the experimental torque - Ψ results (Figures 11 to 13) occurs at about 100% surface shear strain ($\Psi a = 1$). Since the normal stress on the axis, which depends only on $\frac{\partial W}{\partial I_1}$ is a linear function of Ψ^2 up to $\Psi a = 1.3$ (Figures 5 to 10), then $\frac{\partial W}{\partial I_2}$ must be a decreasing function of strain above $\Psi a = 1$. This is not at variance with the linear relationship between t_{zz} and Ψ^2 at the outer hole ($r = 4.31$ cms) in the top plate. The shear strain at $r = 4.31$ cms. is about 110% when the surface shear strain is 130%.

Because the Mooney torque function (2.10) is inadequate to describe the small strain gradient of the exerrimental results, then a corresponding inadequacy between (5.4) and the results is to be expected. The torque predicted by (5.4) is a continuously non-linear function of Ψ. The magnitude and direction of the deviation from linearity depends upon C_2, p, and q. When $p = 0.247$ and $q = 2.18$ then the deviation is in the correct direction if C_2 is positive, and is a maximum when C_2 is a maximum, i.e. when $C_2 = 69$ g.cm^{-2} (Table 5). Then the deviation at $\Psi = 0.3$ is 12 kg.cms. The experimental deviation is 80 kg.cms.

Hart-Smith (1966) proposed strain dependent functions for $\frac{\partial W}{\partial I_1}$, and $\frac{\partial W}{\partial I_2}$ which describe in a qualitative manner the experimental results of Treloar (1944a), and Rivlin and Saunders (1951) over the full range of deformations.

i.e.

$$\frac{\partial W}{\partial I_1} = G \exp[k_1(I_1-3)^2], \quad \frac{\partial W}{\partial I_2} = \frac{Gk_2}{I_2} \qquad (5.8)$$

where G, k_1 and k_2 are constants. G is equal to $\frac{\partial W}{\partial I_1}$ at $I_1 = I_2 = 3$ and represents the stiffness of a particular rubber. Hart-Smith proposes $k_1 = 0.00026$ and $k_2 = 1.2$ to fit the strain variation of

$$\frac{\partial W}{\partial I_1} \text{ and } \frac{\partial W}{\partial I_2}$$

observed by Rivlin and Saunders in their experiments on thin rubber sheets in biaxial extension.

The normal stress t_{zz} and torque M have been obtained by substituting (5.8) into (2.2) and (2.3), using $I_1 = I_2 = 3 + \Psi^2 r^2$.

Then

$$M = \frac{G\pi}{k_1\psi^3}(\exp k_1\psi^4a^4-1) + \frac{2G\pi k_2a^2}{\psi} - \frac{6G\pi k_2}{\psi^3}\ell_n\frac{\psi^2a^2+3}{3} \qquad (5.9)$$

and

$$t_{zz} = G\psi^2\int_{a^2}^{r^2}\exp k_1\psi^4r^4d(r^2) - \frac{2Gk_2\psi^2r^2}{\psi^2r^2+3} \qquad (5.10)$$

which reduces to

$$t_{zz} = \frac{G}{k_1^{\frac{1}{2}}}\left(\text{erfip}_1 - \text{erfip}_2\right) - \frac{2Gk_2\psi^2r^2}{\psi^2r^2+3} \qquad (5.11)$$

where

$$p_1 = k_1^{\frac{1}{2}}\psi^2r^2, \quad p_2 = k_1^{\frac{1}{2}}\psi^2a^2, \text{ and erfi } p = \int_o^p \exp p^2dp \qquad (5.11)$$

Numerical tables of erfi p show that erfi p = p with less than 1% error up to p = 0.16.* (Jahnke, Emde, Losch 1960).

If $k_1 = 0.00026$ then $p_1 = 0.02725$ when $\psi a = 1.3$. Since $p_2 < p_1$ then erfi p_1 and erfi p_2 in (5.11) can be replaced by p_1 and p_2 respectively, and (5.11) becomes

$$t_{zz} = G\psi^2(r^2-a^2) - \frac{2\psi^2r^2Gk_2}{3+\psi^2r^2} \qquad (5.12)$$

Furthermore when $k_1 \ll 1$ then $\exp k_1\psi^4a^4 - 1 \simeq k_1\psi^4a^4$, and (5.9) becomes

$$M = G\pi\psi a^4 + \frac{2G\pi k_2a^2}{\psi} - \frac{6G\pi k_2}{\psi^3}\ell_n\frac{\psi^2a^2+3}{3} \qquad (5.13)$$

If $k_1 = 0.00026$ then (5.12) and (5.13) are applicable. Then the Hart-Smith function (5.8) offer no advantages over the Gent-Thomas stored energy function (5.1) for the description of torsion, because (5.12) and (5.13) are essentially equivalent to (5.3) and (5.4).

---

* It is easy to see that erfi $p \simeq p$ for small values of p by considering the series expansion $\exp p^2 = 1 + p^2 + \frac{p^4}{2} + \ldots$. If p is small so that $p^2 \ll 1$, then erfi $p = \int_o^p 1\,dp = p$.

The constants k_1 and k_2 can be determined from experimental data. The variation of $\frac{\partial W}{\partial I_1}$ with I_1, and $\frac{\partial W}{\partial I_2}$ with I_2, was found by measurements involving the pure homogeneous deformation of thin sheets of (butyl) rubber No. 7. (Table 1 and Figure 4, Hall 1968). The results have been replotted in Figure 31 with axes $\ell n \frac{\partial W}{\partial I_1}$ and $(I_1-3)^2$, or $\frac{\partial W}{\partial I_2}$ and $(I_2)^{-1}$. The straight lines through the points were determined by the least squares method. From the gradient of the lines $k_1 = 0.001$ and G $k_2 = 0.235$. When $I_1 = 3$ then $\ell n \frac{\partial W}{\partial I_1} = \ell n$ G and therefore G = 1.54 kg.cm.$^{-2}$ and $k_2 = 0.153$. When $k_1 = 0.001$ the inadequacies of the Gent-Thomas function are repeated.

An attempt was made to fit the experimental results obtained on rubber No. 7 by using the observed strain dependence of $\frac{\partial W}{\partial I_2}$, i.e. $k_2 = 0.1524$, but altering G and k_1.

G can be found by fitting (5.12) to the normal stress on the axis.

$$\text{at} \quad r = 0, \; t_{zz} = -\psi^2 a^2 G \tag{5.14}$$

and by comparison with the experimental $t_{zz} - \psi^2$ relationship (Figure 5), G = 0.365 kg.cm.$^{-2}$. A value of k_1 ca. 0.9 was obtained by fitting (5.9) to the experimental M - ψ results (Figure 13) at $\psi = 0.1$ and ignoring powers of k_1 higher than k_1^2. However, the strong deviation at (5.9) from linearity is then such that M ca.3500 kg.cms. at $\psi = 0.3$. This is clearly untenable.

In all the foregoing stored energy functions, the values of the material constants chosen to give a good fit between the predicted and experimental normal stress distributions give serious discrepancies between the predicted and experimental torque - ψ relations, and vice versa. It is not easy to reconcile the results with a particular form of stored energy function.

$W(I_1,I_2)$ can be expressed without loss of generality as a power series in I_1 and I_2

$$\text{i.e.} \qquad W = \sum_{p,q=0}^{\infty} A_{pq}(I_1-3)^p(I_2-3)^q \quad \text{where } A_{\infty} = 0 \tag{5.15}$$

If the first three terms of the expansion are considered

$$W = A_{10}(I_1-3) + A_{01}(I_2-3) + A_{11}(I_1-3)(I_2-3) \tag{5.16}$$

If this function describes the torsion results then $\frac{\partial W}{\partial I_1}$ and $\frac{\partial W}{\partial I_2}$ change with

strain at the same rate over the range $3 < I_1 = I_2 < 5$. This is not supported by any experimental evidence. The third material parameter allows an added criterion in the evaluation of the constants. A_1, A_2, and A_3 can be chosen to fit the normal stress at r = o and r = a, and the initial gradient of the M - Ψ results. However, (5.16) then predicts a torque which decreases too rapidly with strain. For example the predicted deviation from linearity at Ψ = 0.2 for rubber No. 7 is 180 kg.cms., compared with the observed deviation of 25 kg.cms.

Excessive curvature in the M - Ψ relationship is similarly obtained if:-

$$W = A_1(I_1-3) + A_2(I_2-3) + A_3(I_2-3)^2 \qquad (5.17)$$

Further attempts to explain the results in terms of a particular stored energy function have been unsuccessful.

5.2 Time dependent rubbers

Isochronous normal stress distributions for rubber No. 6 have been obtained by extracting data at constant time from the stress relaxation curves of Figure 23. Representative distributions obtained after relaxation times of 5, 500, 1000 and 1500 minutes, are shown in Figure 32. A straight line extrapolation of each distribution allowed the normal stress at the edge to be determined and hence $\frac{\partial W}{\partial I_2}$ calculated (2.5). Assuming that $\frac{\partial W}{\partial I_1}$ is independent of strain then $\frac{\partial W}{\partial I_1} = A$ can be calculated from the normal stress on the axis (2.4).

It is apparent that the normal stress axis decreases more rapidly than the normal stress at the edge. This is claarly seen in Figure 33 in which A and $\frac{\partial W}{\partial I_2}$ are plotted against a logarithmic time axis. The Mooney parameters C_1 and C_2 for each isochronous distribution were obtained, as in section 5 1 from the straight line relationship between t_{zz}/Ψ^2 and a^2-r^2, and are also plotted against time in Figure 33. It is interesting to observe that $\frac{\partial W}{\partial I_2} \simeq C_2$ over the complete time range, and reduces to a constant value of about 65. g.cm^{-2} after about 200 minutes, although A and C_1 are continuously decreasing functions of time.

In an attempt to explain the stress relaxation in terms of the time dependence of the stored energy function, the constitutive equation of state developed by Kaye (1962) for an incompressible viscoelastic liquid has been modified to describe a viscoelastic solid.

If an instantaneous torsional deformation is applied to an incompressible viscoelastic liquid a time t = o, then according to Kaye (1963)

$$t_{zz} = 2\psi^2 \int_a^r \int_{-\infty}^{0} \frac{\partial \Omega}{\partial J_1} dt' dr - 2\psi^2 r^2 \int_{-\infty}^{0} \frac{\partial \Omega}{\partial J_2} dt' \qquad (5.18)$$

and

$$M = 4\pi\psi \int_0^a r^3 \left[\int_{-\infty}^{0} \frac{\partial \Omega}{\partial J_1} dt' + \int_{-\infty}^{0} \frac{\partial \Omega}{\partial J_2} dt' \right] dr \qquad (5.19)$$

where $J_1 = J_2 = 3 + \psi^2 r^2$ and t' is some past time. The current time is denoted by t.

Ω is a function of J_1, J_2 and the elapsed time $t-t'$, and by analogy with the elastic stored energy function, can be represented by a power series

$$\Omega = \sum_{p,q=0}^{\infty} B_{pq}(J_1-3)^p(J_2-3)^q \quad \text{where } B_{oo} = 0 \qquad (5.20)$$

The parameters tend to zero as $t-t'$ tends to infinity. Following a previous Note, (Hall, 1968), it is reasonable to consider that a viscoelastic solid may be represented by

$$\Omega = B_{1o}(J_1-3) + B_{o1}(J_2-3) \qquad (5.21)$$

where B_{1o} and B_{o1} are decreasing functions of $t-t'$, which are finite as $t-t'$ approaches infinity.

For example:

$$B_{1o} = A' e^{\alpha t'} + B e^{-k_1(t-t')} \qquad (5.22)$$

and

$$B_{o1} = C e^{\beta t'} + D e^{-k_2(t-t')}$$

then

$$t_{zz} = \psi^2 \left(\frac{A'}{\alpha} + \frac{B}{K_1} e^{-k_1 t} \right)(r^2-a^2) - 2\psi^2 r^2 \left(\frac{C}{\beta} + \frac{D}{K_2} e^{-k_2 t} \right) \qquad (5.23)$$

and

$$M = \pi\psi a^4 \left(\frac{A'}{\alpha} + \frac{C}{\beta} + \frac{B}{K_1} e^{-k_1 t} + \frac{D}{K_2} e^{-k_2 t} \right) \qquad (5.24)$$

If the normal stress distribution for an elastic rubber can be described quantitatively by (2.9), that is, by using the Mooney stored energy function, then from (5.23), measured values of C_1 and C_2 under non-equilibrium conditions are such that

$$C_1 = \frac{A'}{\alpha} + \frac{B}{k_1} e^{-k_1 t} \qquad (5.25)$$

and

$$C_2 = \frac{C}{\beta} + \frac{D}{k_2} e^{-k_2 t} \qquad (5.26)$$

C_1 and C_2 are plotted on a logarithmic scale as functions of the relaxation time in figure 34. C_2 decreases to a minimum of about 60 g.cm^{-2} in the range 200 minutes < t < 400 minutes, and then $\ell n C_2$ increases in a linear manner with time. At t = 1500 minutes then C_2 = 70 g.cm^{-2}. This may reflect the inadequacy of the Mooney function. The corresponding values of $\frac{\partial W}{\partial I_2}$ found by the straight line extrapolation of the normal stress distribution decreases to a constant value of about 66 g.cm^{-2} in about 300 minutes.

If

$$\frac{\partial W}{\partial I_2} = \frac{C}{\beta} + \frac{D}{k_2} e^{-k_2 t} \qquad (5.27)$$

then

$$\frac{C}{\beta} = \left(\frac{\partial W}{\partial I_2}\right)_{t=300}$$

and

$$\ell n \left[\left(\frac{\partial W}{\partial I_2}\right)_t - \left(\frac{\partial W}{\partial I_2}\right)_{t=300} \right] = \ell n \frac{D}{k_2} - k_2 t \qquad (5.28)$$

$\left(\frac{\partial W}{\partial I_2}\right)_t - \left(\frac{\partial W}{\partial I_2}\right)_{t=300}$ is plotted in figure 34 on a logarithmic scale, against time.

The linear relationship suggested by (5.28) is observed, with D/k_2 = 18 g.cm^{-2} and k_2 = 0.207 minutes^{-1}.

The linear relationship between ℓ n C_1 and t suggests that $A'/\alpha = 0$ (5.25). Then $B/k) = 490$ g.cm^{-2} and $k_1 = 3.9.10^{-4}$ minutes^{-1}, and (5.25) suggests that C_1 will decrease to 67 g.cm^{-2}

$\left(\simeq \frac{\partial W}{\partial I_2}\right)$ in 5000 minutes.

In common with observations on the elastic rubbers there is a difference in the magnitude of $C_1 + C_2$ determined from the torque - Ψ relationship and $C_1 + C_2$ determined from the normal stress measurements. (Figure 33 and Table 7).

Rubber No.	2 minute time interval		10 minute time interval	
	$(C_1+C_2)_{n.s.}$	$(C_1+C_2)_t$	$(C_1+C_2)_{n.s.}$	$(C_1+C_2)_t$
1	1324	1815		
2	1596	2050	1649	2030
3	1814	2555	1758	2555
4	1086	1400	1035	1400
5	1194	1695	1197	1695
7			849	1315

Table 7. (C_1+C_2) determined from normal stress (n.s.) and torque (t) measurements for increasing strains. The units of (C_1+C_2) are $kg.cm^{-2}$.

The difference between the two values of C_1+C_2 for each rubber has been plotted against a function of the rubber stiffness (Figure 35). The stiffness criterion was chosen to be C_1+C_2 obtained from the $M - \Psi$ results after a 10 minute relaxation time at a strain $\Psi a = 1.3$. Figure 35 suggests that the discrepancy will disappear for very lightly crosslinked rubbers. Attempts to explain the phenomena in terms of a stored energy function have failed (Section 5.1).

The total normal force N acting over the end plates of a Mooney rubber sample is dependent on C_1+2C_2. (2.14), and N is proportional to the axial movement in the bearings supporting the sample. It is therefore possible that the discrepancy disappears when the axial movement is zero, and the importance of the bearing movement, discussed in section 3.2.2., was underestimated.

6. Summary and conclusions

The analysis of the results can be summarised into four major groups.

1. The normal stresses acting over the end surfaces of a right circular cylinder of radius a are such that a linear relationship between the normal stress, and radial position r is necessary, in the range $r > 0.6\ a$, to describe the isochronous normal stress distribution for all the rubbers. Extrapolation to the edge of the samples for rubbers which exhibit little or no stress relaxation, reveals a finite value for $\frac{\partial W}{\partial I_2}$. Curvature in the torque-strain relationship demonstrates the inadequacy of the Mooney stored energy function. It is shown that the Hart-Smith and Gent-Thomas stored energy functions are essentially the same for the strain range encountered in torsion. Both functions are inadequate to describe the normal stress and the torque measurements. Attempts to describe the

complete equilibrium stress system by a particular stored energy function were unsuccessful.

2. The advantages offered by the cone and plate system for the extrapolation of the normal stress distribution were completely offset by difficulties in sample preparation. Within these limitations however, the normal stress is a logarithmic function of the radius, in accordance with theory, and the normal stress at the edge, and hence $\frac{\partial W}{\partial I_2}$, is finite.

3. Stress relaxation measurements upon a lightly crosslinked natural rubber in torsion show that there is an exponential reduction of $\frac{\partial W}{\partial I_1}$ and $\frac{\partial W}{\partial I_2}$ with time, in accordance with a proposed energy function which may be considered the viscoelastic equivalent of the Mooney elastic stored energy function. $\frac{\partial W}{\partial I_1}$ reduces to a finite constant value although the normal stress and $\frac{\partial W}{\partial I_1}$ are continuously decreasing.

4. Heat build up during torsion could be misinterpreted as a time dependent C_2 term in the stress strain relationships. However conduction effects ensure that this contribution to a measured C_2 reduces almost to zero in a time period less than the time scale of the experiments.

The finite value of $\frac{\partial W}{\partial I_2}$ which was observed under quasi-elastic conditions, and as the limiting value of the time dependence of $\frac{\partial W}{\partial I_2}$ clearly supports the hypothesis that the kinetic theory of elasticity is unable to describe fully the elastic behaviour of the rubber in a state of finite deformation. This supports previous evidence obtained on measurements of sheet rubber in a state of pure homogeneous deformation. (Hall, 1968).

Major difficulties in the interpretation of the torsion results have occurred because of the discrepancies in the values of C_1+C_2 determined from the normal stress and torque. In order to eliminate completely the possibility of effects due to axial expansion of the sample, in future work, the supporting bearing should have a different internal geometry, such as a flat thrust bearing.

Photoelastic methods for the determination of the normal stress distributions were considered, and rejected in favour of specially designed dynamometers. It has been pointed out, however, that a polarimeter has recently become available which, after modification, may be capable of a rapid determination of the normal stress at a large number of positions across the sample end surface. This system merits further investigation. It should be possible to determine the normal stress distribution very accurately for a wide range of elastomers. Temperature effects and rubber-filler systems could be examined.

Appendix 1

The torsion of a cone and plate sample

The approach to the problem is that of Kaye (1962) who considered the flow of a viscoelastic liquid between a rotating and a touching stationary plate. Kaye developed relationships between the stress, and a strain function which relates the deformation at the present time with that at some past time. His equations have been modified to describe an incompressible elastic solid. These equations are only exact if the boundary surface of the rubber is a sphere centred on the cone apex. If the boundary surface is cylindrical then errors will be small if η is small where the semi-vertical angle of the cone is $\pi/2 - \eta$.

Let the cartesian coordinate axis x_3 coincide with the sample axis and the coordinate origin 0 be the cone apex. Then any point $P(x_1,x_2,x_3)$ in the deformed material can be represented in spherical polar coordinates (r, θ, ϕ) by the transform

$$\begin{aligned} x_1 &= r \cos\phi \sin\theta \\ x_2 &= r \sin\phi \sin\theta \\ x_3 &= r \cos\theta \end{aligned} \qquad (A.1)$$

If the cone had been twisted through an angle β then OP was twisted through $\beta/\eta(\frac{\pi}{2} - \theta)$. Therefore the position (x_1', x_2', x_3') of P in the unstrained sample is given by

$$\begin{aligned} x_1' &= r \cos\left[\phi - S(\tfrac{\pi}{2} - \theta)\right]\sin\theta \\ x_2' &= r \sin\left[\phi - S(\tfrac{\pi}{2} - \theta)\right]\sin\theta \\ x_3' &= r \cos\theta \end{aligned} \qquad (A.2)$$

where $S = \beta/\eta$. The equation of state proposed by Kaye can be written for an elastic material as:

$$\sigma_{ij} - \sigma\delta_{ij} = 2\left[\frac{\partial W}{\partial I_1}\left(h_i h_j \frac{\partial\theta_i}{\partial x_\alpha'}\frac{\partial\theta}{\partial x_\alpha'}\right) - \frac{\partial W}{\partial I_2}\left(\frac{1}{h_i h_j}\frac{\partial x_\alpha'}{\partial\theta_i}\frac{\partial' x_\alpha}{\partial\theta_j}\right)\right] \qquad (A.3)$$

where i and j take the values 1, 2, or 3 and the repeated suffix α implies summation. σ_{ij} is the stress tensor and $\sigma\delta_{ij}$ is a hydrostatic stress. I_1 and I_2 and the invariants of the strain tensor δ_{ij} where

$$S_{ij} = h_i h_j \frac{\partial\theta_i}{\partial x_\alpha'}\frac{\partial\theta_j}{\partial x_\alpha'} \qquad (A.4)$$

so that $I_1 = S_{kk}$ $I_2 = \frac{1}{2}(S_{kk} - S_{kl}\,S_{lk})$ and $I_3 = \det S_{ij}$ (A.5)

The coordinates θ_i represent r, θ and ϕ and the parameters h_i are defined by

$$dx_1^2 + dx_2^2 + dx_3^2 = h_1^2 dr^2 + h_2^2 d\theta^2 + h_3^2 d\phi^2 \tag{A.6}$$

Then from (A.2), (A.4), (A.5) and (A.6)

$$I_1 = I_2 = 3 + S^2\sin^2\theta \text{ and } I_3 = 1. \tag{A.7}$$

Substituting (A.2) and (A.6) into (A.3) gives

$$(\hat{rr}) - \sigma = 2\left[\frac{\partial W}{\partial I_1} - \frac{\partial W}{\partial I_2}\right]$$

$$(\hat{\theta\theta}) - \sigma \qquad \left[\frac{\partial W}{\partial I_1} - \frac{\partial W}{\partial I_2}(1 + S^2\sin^2\theta)\right]$$

$$(\hat{\phi\phi}) - \sigma = 2\left[\frac{\partial W}{\partial I_1}(1+S^2\sin^2\theta) - \frac{\partial W}{\partial I_2}\right]$$

$$(\hat{\theta\phi}) = -2\,S\sin\theta\,\left(\frac{\partial W}{\partial I_1} + \frac{\partial W}{\partial I_2}\right) \tag{A.8}$$

$$(\hat{r\theta}) = (r\phi) = 0$$

The components of the stress tensor have been expressed in the usual polar coordinate notation. The equations of motion when inertial and body forces are ignored are (Love, 1944).

$$\frac{\partial(\hat{rr})}{\partial r} + \frac{1}{r}\frac{\partial(\hat{r\theta})}{\partial\theta} + \frac{1}{r\,\mathrm{Sin}\,\theta}\frac{\partial(\hat{r\phi})}{\partial\phi} + \frac{1}{r}\left[2(\hat{rr}) - (\hat{\theta\theta}) - (\hat{\phi\phi}) + (\hat{r\theta})\cot\theta\right] = 0$$

$$\frac{\partial(\hat{r\theta})}{\partial r} + \frac{1}{r}\frac{\partial(\hat{\theta\theta})}{\partial\theta} + \frac{1}{r\sin\theta}\frac{\partial(\hat{\theta\phi})}{\partial\phi} + \frac{1}{r}\left[\left\{(\hat{\theta\theta}) - (\hat{\phi\phi})\right\}\cot\theta + 3(\hat{r\theta})\right] = 0$$

$$\frac{\partial(\hat{r\phi})}{\partial r} + \frac{1}{r}\frac{\partial(\hat{\theta\phi})}{\partial\theta} + \frac{1}{r\sin\theta}\frac{\partial(\hat{\phi\phi})}{\partial\phi} + \frac{1}{r}\left[3(\hat{r\phi}) + 2(\hat{\theta\phi})\cot\theta\right] = 0 \tag{A.9}$$

It can be shown that (A.8) when inserted (A.9) are compatible when $\theta = \frac{\pi}{2}$.

Then

$$\frac{\partial \sigma}{\partial r} + \frac{2s^2}{r}\left(\frac{\partial W}{\partial I_2} - \frac{\partial W}{\partial I_1}\right) = 0$$

$$\frac{1}{r}\frac{\partial \sigma}{\partial \theta} = 0$$

$$\frac{\partial \sigma}{\partial \phi} = 0 \qquad \text{(A.10)}$$

Equations (A.10) will therefore be an approximate solution of (A.9) when α is small. If $(\hat{rr}) = 0$ when $r = a$, then from (A.8) and (A.10)

$$\sigma = 2s^2\left(\frac{\partial W}{\partial I_1} - \frac{\partial W}{\partial I_2}\right)\ell n\,\frac{r}{a} - 2\left(\frac{\partial W}{\partial I_1} - \frac{\partial W}{\partial I_2}\right) \qquad \text{(A.11)}$$

and hence by substitution of (A.11) into (A.8) when $\theta = \frac{\pi}{2}$, the stress normal to the plate at the radial position r is given by

$$t_{zz} = (\hat{\theta\theta}) = -2s^2\left(\frac{\partial W}{\partial I_1} - \frac{\partial W}{\partial I_2}\right)\ell n\,\frac{a}{r} - 2s^2\frac{\partial W}{\partial I_2}\Big) \qquad \text{(A.12)}$$

and the torque

$$N = \int_0^a 2\pi(\hat{\theta\phi})r^2 dr = \frac{4}{3}\pi a^3 s\left(\frac{\partial W}{\partial I_2} + \frac{\partial W}{\partial I_2}\right) \qquad \text{(A.13)}$$

hence at the edge of the sample

$$(t_{zz})_{r=a} = -2s^2\frac{\partial W}{\partial I_2} \qquad \text{(A.14)}$$

It should be noted from (A.7) that I_1 and I_2 are independent of r. Therefore $\frac{\partial W}{\partial I_1}$ and $\frac{\partial W}{\partial I_2}$ are also independent of r since W is a function of I_1 and I_2 only. Then for any given twist S (A.12) suggests that there is a linear relationship between t_{zz} and $\ell n\ a/r$ whatever the form of the stored energy function.

Appendix 2

Sample preparation and characterisation

2.1 Sample preparation

All the samples were prepared under controlled conditions. The detailed recipes are given in Table 8, in which the numbers denote parts by weight.

Rubber No.	1	2	3	4	5	6	7
Natural rubber	100	100	100	100	100	100	-
Butyl rubber (Esso grade 218)	-	-	-	-	-	-	100
Sulphur	2	3	5	-	-	-	2
Zinc oxide	5	5	5	-	-	-	5
Stearic acid	1	1	1	-	-	-	3
Antioxidant	1	1	1	-	-	-	-
Accelerator	1	1	1	-	-	-	1.5
Dicumyl peroxide	-	-	-	2	3	0.5	-

Table 8. The sample recipe.

The holes in the flat metal end plates of the torsion samples were plugged and then machine ground to a good surface finish.

The end plates for the parallel plate samples were coated with a bonding agent (Chemlok 220, Durham Chemical Company) in such a manner as to ensure that bonding occurs over the plates, but not over the plug surfaces. The end plates and rubber mix were contained in a suitable mould. After curing under pressure for thirty minutes at 150°C the plugs were removed to expose a free rubber surface. It is this surface which bulges during torsion. Further machining of the completed samples ensures that the end plates are parallel to each other to within 10^{-3} cms.

Rubber for the cone and plate system was vulcanised between the appropriate end plates. No bonding agent was used. Bonds formed by vulcanisation at 150°C would have created strains of about 30% in the rubber because of the differential thermal contraction of rubber and metal. The rubber was bonded to the end plates at room temperature using a cyanoacrylate adhesive (Eastman 910, CIBA Ltd.).

Anisotropy and inhomogeneity was examined by swelling measurements. Equilibrium swollen lengths were observed for rubber cut from various positions and orientations in the samples. The maximum swelling variations was 0.2% which, from observed relationships between swelling and modulus, is equivalent to modulus variations of less than 5% (Hall, 1968).

2.2 Sample characterisation

The natural rubber samples were characterised by finding an average molecular weight, M_c, for the polymer chain between adjacent network junctions. Then M_c^{-1} will be a measure of the density of crosslinks in the rubber matrix.

Flory (1942) and Huggins (1942) separately derived an expression for the free energy of dilution of a polymer in a liquid. At any given temperature their expressions are the same.

Using the kinetic theory stored energy function it can be shown (Treloar 1958) that for an equilibrium degree of swelling

$$M_c^{-1} = \frac{-\ell n(1-v_r) - v_r - \mu v_r^2}{\rho V v_r^{1/3}} \qquad (A.15)$$

where v_r is the volume fraction of rubber in the mixture, ρ is the density of rubber, V is the molar volume of the liquid, and μ is an interaction constant for the liquid-rubber mixture.

Sections of the samples were swollen in benzene and the equilibrium weights determined. The parameter μ was taken to be 0.42 (Gumbrell, Mullins and Rivlin, 1953). The calculated values of M_c^{-1} are given in Table 9.

Rubber No.	$M_c^{-1} \times 10^4$
1	1.36
2	1.76
3	2.27
4	1.39
5	1.66
6	0.44

Table 9. $(M_c)^{-1} \times 10^4$, for rubber taken from the different test pieces.

Simple extension measurements were made on dumbell shaped samples cut from thin sheets of rubber which had crosslink densities similar to the rubbers used in torsion.

Using the test procedure and method of analysis of Rivlin and Saunders (1951) the variation with $1/\lambda$ of the function

$$\frac{\partial W}{\partial I_1} + \frac{1}{\lambda}\frac{\partial W}{\partial I_2}$$

was calculated and is given in Table 10 and Figure 36. In order to characterise the rubber mechanically, and to provide design data for the torsion equipment, the values of $\frac{\partial W}{\partial I_1}$ and $\frac{\partial W}{\partial I_2}$ have been calculated. The magnitude of $\frac{\partial W}{\partial I_1} + \frac{\partial W}{\partial I_2}$ for each rubber is given by the extrapolation of the linear

section of each curve to the $^1/\lambda = 1$ ordinate, and $\frac{\partial W}{\partial I_2}$ is the gradient of the linear section. The values of $\frac{\partial W}{\partial I_1}$ and $\frac{\partial W}{\partial I_2}$ are given in Table 11.

Appendix 3

The error involved in the method of calculation of the normal stress

The normal stress at the centre of a hole in the end plate of a sample is calculated as the force exerted by the dynamometer plunger to restrain bulging divided by the effective cross-sectional area of that plunger. This assumption is only accurate if the normal stress is constant over the area of the plunger.

The error has been calculated for a parabolic normal stress distribution (The Mooney distribution (2.9)). Consider a plunger of effective radius d at a radial distance b from the axis of the torsion sample.

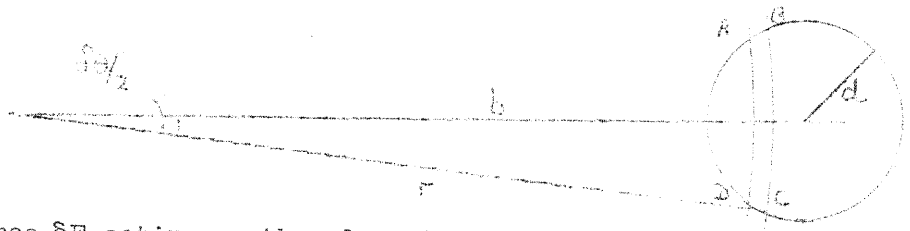

The force δF acting on the element of area ABCD in the diagram is given by

$$\delta F = t_{zz}\, r\delta\theta\, .\delta r \qquad (A.16)$$

where t_{zz} is the normal stress at a radial distance r. δr is an infinitesimal increment in r, and

$$\delta\theta = 2\cos^{-1}\frac{b^2+r^2-d^2}{2br} \qquad (A.17)$$

Therefore the total force F acting on the plunger is given by

$$F = \int_{b-d}^{b+d} t_{zz}\, 2r\cos^{-1}\frac{b^2+r^2-d^2}{2br}\, .dr \qquad (A.18)$$

If t_{zz} is given by the Mooney distribution (2.9) then evaluation of the subsequent integral gives

$$F = \pi\psi d^2(C_1-2C_2)\left(b^2+\frac{d^2}{2}\right) - \pi\psi^2 d^2 a^2 C_1 \qquad (A.19)$$

The calculated normal stress t'_{zz} is defined as $F/\pi d^2$ and therefore

$$t'_{zz} - \psi^2(C_1-C_2)(b^2+\frac{d^2}{2}) - {}^2a^2C_1 \qquad (A.20)$$

The true normal stress t_{zz} at the centre of the olunger is given by (2.9) when r = b and hence the error in the calculated normal stress is

$$t'_{zz} - t_{zz} = -\frac{\psi^2 d^2}{2}(C_1-2C_2) \qquad (A.21)$$

The error for a given strain is therefore independent of the radial position and is a maximum when (C_1-2C_2) is a maximum. It is easy to show that the maximum value of the relative error $(t'_{zz} - t_{zz})/t_{zz}$ occurs when C_1/C_2 is a maximum. Using the increasing strain values of C_1 and C_2 from Table 3 $(C_2 = \frac{\partial W}{\partial I_2})$ then the maximum percentage error occurs for rubber No. 4 and is about 0.3% on the sample axis increasing to 2% at the edge. These errors are negligible compared with the errors involved in extrapolating the distribution to the edge.

Appendix 4

The evolution and conduction of heat in the samples

(i) The evolution of heat in the parallel plate torsion sample

The temperature build up in the sample during torsional deformation has been estimated by finding the heat equivalent of the mechanical work done assuming no internal energy changes.

According to Rivlin (1948b) the tangential stress $t_{\theta z}$ acting on the end surface of the cylinder at a radial distance r is given by

$$t_{\theta z} = 2\psi r\left(\frac{\partial W}{\partial I_1} + \frac{\partial W}{\partial I_2}\right) \qquad (A.22)$$

where ψ is the angle of twist per unit length.

The moment about the axis of the tangential force acting on the element of area $2\pi r dr$ is therefore

$$4\pi\psi r^3\left(\frac{\partial W}{\partial I_1} + \frac{\partial W}{\partial I_2}\right)dr \qquad (A.23)$$

and the work done in twisting a hollow cylinder of unit length, radius r and wall thickness dr through ψ radians is given by

$$\delta W = \int_0^{\psi} \left[4\pi\psi r^3 \left(\frac{\partial W}{\partial I_1} + \frac{\partial W}{\partial I_2} \right) dr \right] d\psi \qquad (A.24)$$

$$= 2\pi\psi^2 r^3 (C_1+C_2) dr$$

assuming that for a given value of r $\frac{\partial W}{\partial I_1}$ and $\frac{\partial W}{\partial I_2}$ are independent of ψ and equal to C_1 and C_2 respectively.

If δQ is the heat build up in the hollow cylinder

$$\delta W.g = J.\delta Q = J.\delta m.c.\delta T \qquad (A.25)$$

where

$J = 4.185 \ .10^7 \text{ergs.cal}^{-1}$

δm = mass of the cylinder of density ρ, $= 2\pi r dr \rho$

c = specific heat of the sample

δT = (finite) rise in temperature, °C

$g = 981 \text{ cm.sec}^{-2}$

$$\therefore \delta T = \frac{(C_1+C_2)}{J\rho c} g.\psi^2 r^2 \qquad (A.26)$$

Therefore there is a parabolic temperature distribution through a rapidly deformed solid cylinder. This distribution is in error if

$$\frac{\partial W}{\partial I_1} \text{ and } \frac{\partial W}{\partial I_2}$$

are functions of strain and temperature but (A.26) is sufficiently accurate to allow an estimation of the magnitude of δT.

For a well vulcanised natural rubber gum typical values of the parameters in (A.26) are

$C_1 + C_2 = 2 \text{ kg.cm}^{-2}$

$\rho = 0.95 \text{ g.cm}^{-3}$

$\tau = 0.47 \text{ cal.g}^{-1}.°C^{-1}$

The temperature rise at the edge of the sample for a 130% surface shear strain is then about 0.18°C. The average temperature rise in the sample of radius a is given by

$$\bar{\delta T} = \frac{(C_1+C_2) g.\psi^2 a^2}{2J\rho c} \qquad (A.27)$$

and is about 0.9°C for this typical rubber at the same strain. According to the kinetic theory of elasticity

$$\frac{\partial W}{\partial I_1} = C_1 = NkT \qquad (A.28)$$

and therefore a temperature increase of 0.9°C above the ambient temperature will alter C_1 by about 0.03%. This is of negligible significance.

It is interesting to note that the temperature distribution can give a finite time dependent value for $\frac{\partial W}{\partial I_2}$. The heat evolved during deformation will be lost by conduction and radiation and therefore (A.26) can be written

$$\delta T(t) = B(t)\psi^2 r^2 \qquad (A.29)$$

where $\delta T(t)$ and $B(t)$ are functions of time and $B(o) = \frac{C_1+C_2}{J\rho c}.g$

If the ambient temperature T is increased by δT then an apparent value for $\frac{\partial W}{\partial I_1}$ is given by

$$\frac{\partial W}{\partial I_1} = Nk(T+\delta T) = C_1 + NkB(t)\psi^2 r^2 \qquad (A.30)$$

For torsion $I_1 = I_2 = 3 + \psi^2 r^2$ and hence $\psi^2 r^2$ can be expressed as a function of I_1, a function of I_2, or a function of I_1 and I_2.

For example $\psi^2 r^2$ can be expressed as $(I_1-3)^i(I_2-3)^j$ where i and j can have any values which satisfy the condition $i + j = 1$.

Then integrating (A.30) with respect to I_1

$$W = C_1(I_1-3) + \frac{NkB(t)}{(i+1)}(I_1-3)^{i+1}(I_2-3)^j \qquad (A.31)$$

and hence

$$\frac{\partial W}{\partial I_2} = \frac{j}{2-j} NkB(t)(I_1-3)^{i+1}(I_2-3)^{j-1} \qquad (A.32)$$

Therefore these functions will provide a finite value for $\frac{\partial W}{\partial I_2}$ (unless $j = o$) which will be larger if j has a value close to 2 and will become zero only when the temperature increase δT has decayed to zero.

(ii) The conduction of heat from the parallel plate sample

Most of the heat lost from the sample is by conduction into the metal end plates. If the small amount of heat lost by radiation over the curved surface is ignored, then the equation describing heat flow is

$$\frac{\partial T}{\partial t} = \frac{K}{\rho c} \frac{\partial^2 T}{\partial z^2} \qquad (A.33)$$

where T is the temperature at time t. K is the thermal conductivity of the rubber and z is the direction parallel to the sample axis.

The solution of (A.33) must satisfy certain initial and boundary conditions. It is convenient to use a temperature scale with ambient temperature as zero. Then at time t = 0 the sample temperature is $\delta T(0)$ which is indepent of z. The metal end plates are attached to the torsion jig and the mass of metal involved is such that the end plates can be considered to remain at the ambient (zero) temperature.

Then according to Carslaw and Jaeger (1959) the sample temperature at any time $\delta T(t)$ is given by

$$\delta T(t) = \delta T(0) - \delta T(0) \sum_{n=0}^{\infty} (-1)^n \left[\operatorname{erfc} \frac{(2n+1)\ell - z}{2(kt)^{\frac{1}{2}}} + \operatorname{erfc} \frac{(2n+1)\ell + z}{2(kt)^{\frac{1}{2}}} \right] \qquad (A.34)$$

where $-\ell < z < \ell$ and $k = \frac{K}{\rho c}$. $\delta T(t)$ is represented grapically in Figure 37 (i) $\delta T(0)$ is equal to $\rho c B(0) \Psi^2 r^2$.

The average temperature $\overline{\delta T}$ in the sample at time t is given by

$$\overline{\delta T}(t) = \overline{\delta T}(0) - 2\overline{\delta T}(0) \left(\frac{kt}{\ell^2} \right)^{\frac{1}{2}} \left[\frac{1}{\pi^{\frac{1}{2}}} + 2 \sum_{n=1}^{\infty} (-1)^n \operatorname{ierfc} \frac{n\ell}{(kt)^{\frac{1}{2}}} \right] \qquad (A.35)$$

where $\overline{\delta T}(0)$ is the average sample temperature at time t = 0 and $\overline{\delta T}(0) > \overline{\delta T}(t)$. $\overline{\delta T}(t)$ is shown graphically in figure 37 (ii).

Appendix 5

The measurement of the normal stress distribution by photo-elastic methods

Calculations have been made to consider the feasability of measuring the normal stress distribution by examining the isochromatic fringe pattern formed in a plate of stressed transparent materials.

The material would be placed so that it stopped the rubber bulging into a slot made along a diameter of the metal end plate.

A brief outline of photoelastic behaviour and the relevant calculations are detailed below.

Stress applied to an isotropic transparent material will produce a double refraction effect in that material. Under the action of a compressive stress the material will behave like a uniaxial crystal and polarised light incident in a direction perpendicular to the optic axis of the crystal will be split into two components parallel and normal to the optic axis. The relative retardation of these to components as they pass through the material is proportional to the thickness of the material and the applied stress. The constant of proportionality is called the stress-optical coefficient.

If the stress-optical coefficient of the material is known then measurement of the relative optical retardation will therefore allow determination of the magnitude of the applied stress.

Consider a strip of photoelastic material of length ℓ and with a rectangular cross-section of width w and thickness d. If a compressive stress p acting on the strip produces a relative retardation of x wave length of the incident monochromatic light of wavelength.

$$\text{The } x = Cpd \qquad \text{(A.50)}$$

where C is the stress-optical coefficient.

If the dimensions of the strip are such that the normal stress t_{zz} acting over the cross-sectional area can be assumed to be constant, then

$$x = \frac{t_{zz}\, d}{f} \qquad \text{(A.51)}$$

where $f = \frac{\lambda}{C}$

The smallest stress to be measured is at the edge of the rubber cylinder. If the rubber material parameter C_2 is assumed to be 0.1 $kg.cm^{-2}$, and Ψ is 0.3 radians cm^{-1} (an angle of twist of the sample of 5°) then from (4.12) the stress at the edge is about 18 $g.cm^{-2}$. If this compressive stress acts on a strip of photoelastic material of thickness 1 cm. and fringe value f equal to 12 $kg.cm^{-1}$ (Araldite CT 200 epoxy resin) then according to (A.51) the retardation is approximately 15.10^{-4} fringe widths. The maximum retardation will occur on the axis of the sample and is unlikely to be more than 0.3 fringe widths. Hence a photograph of the complete fringe system over the diameter of the cylinder will not allow a sensitive evaluation of the stress distribution.

Local regions of the photoelastic plate could be examined by a polarimeter but the lower limit of sensitivity of an optical compensator such as the Senarmont is about 5.10^{-3} fringe widths (Jerrard and McNeil, 1960).

The sensitivity could be increased considerably by using the compensator in a darkened room in conjunction with a half shadow plate but this was considered inconvenient and the dynamometer described in section 5.3.1 was designed.

The changes in length of the photoelastic plate under the compressive stress are negligible but errors due to the stress relaxation within the plate would have to be considered. Converting the plate into a number of discrete strips would be advisable to minimise strain interference in the material.

A commercial polarimeter using photocells is now available (the Bendix N.P.L. automatic polarimeter Type 700A) and is described in the Physics Handbook (1966). It claims a lower limit of sensitivity of about 10^{-6} fringe widths, but in its present form is limited to a range of about $\pm 15.10^{-4}$ fringes. It is possible to modify the instrument so that it will measure $\pm 15.10^{-4}$ fringes from a manually pre-set position, without loss of sensitivity. The overall sensitivity of the required range for normal stress measurement will therefore be controlled by the ability to off-set the polarizer and analyser by a predetermined amount. This instrument used in conjunction with a photoelastic material such as epoxy resin may now facilitate an easy and rapid determination of the normal stress distribution.

References

1. Carslaw and Jaeger (1959) — Conduction of heat in Solids (2nd ed.)
2. Ciferri and Flory — Jnl. App. Phys., 1959, 30(10), 1498
3. Flory — Jnl. Chem. Phys. 1942, 10, 51.
4. Gent and Thomas — Jnl. Pol. Sci. 1958, 28, 625.
5. Gumbrell, Mullins, and Rivlin — Trans. Far. Soc. 1953, 49(12), 1495.
6. Hall — College of Aeronautics Note Mat. 16, 1968.
7. Hart-Smith — Z.A.M.P., 1966, 17, 5, 608.
8. Huggins — Am. N.Y. Acad. Sci. 1942, 43, 1.
9. Jahnke, Emde, and Losch — Tables of Higher Functions, McGraw Hill, 1960.
10. Jerrard and McNeil — Theoretical and Experimental Physics. Chapman and Hall, 1960.
11. Kaye — C. of A. Note No. 134, 1962.

12.	Kaye	C. of A. Note No. 149, 1963.
13.	Love	The Mathematical Theory of Elasticity.
14.	Mooney	Jnl. App. Phys. 1940, 11, 582.
15.	Mooney	Jnl. App. Phys. 1964, 35(1), 23.
16.	Rivlin	Phil. Trans. 1948a, A 240, 459.
17.	Rivlin	Phil. Trans. 1948b, A.241, 379.
18.	Rivlin	Phil. Trans. 1949a, A.242, 173.
19.	Rivlin	Proc. Camb. Phil. Soc. 1949, 45, 485.
20.	Rivlin	Rheology. 1956, 1, 351. Academic Press, 1956.
21.	Rivlin and Saunders	Phil. Trans. Roy. Soc. 1951, A.243, 251.
22.	Treloar	Trans. Far. Soc. 1944a, 40, 109.
23.	Treloar	The Physics of Rubber Elasticity, 2nd. ed. Clarendon Press, 1958.

Acknowledgement

The author is pleased to acknowledge the frequent valuable discussions with Professor D.W. Saunders.

The test equipment was built by the workshop staff of the Department of Materials.

The rubber samples were prepared by Mr. J.M. Stuart.

Table 1 The variation of normal load with ψ, at various radial positions over the end plates of the parallel plate samples. All loads measured after two minutes at each strain increment

Hole A is at radial position r = 4.31 cms; hole B at r = 3.68 cms; hole C at r = 3.05 cms, hole D at r = 2.47 cms, hole E at r = 0 cms; sample radius a = 5.05 cms. N(gms) at A is the load applied to the plunger mounted centrally in hole A. The normal stress at the centre of the hole is N ÷ 0.51 cm^2

Sample	ψ rad. cm^{-1}	ψ^2 rad^2 cm^{-2}	N(gms) at A increasing strain	N(gms) at A decreasing strain	N(gms) at B incr. strain	N(gms) at B decr. strain	N(gms) at C incr. strain	N(gms) at C decr. strain	N(gms) at D incr. strain	N(gms) at D decr. strain	N(gms) at E incr. strain	N(gms) at E decr. strain	Torque (kg. cms) incr. strain	Torque (kg. cms) decr. strain
	0.0289	0.0008	15±0	(1 set of	10±10		15±5		15±5		12±7		104±14	58±2
	0.0579	0.0033	25±0	results	22±2	25±25	52±12	5±5	42±7	30±30	50±2		205±5	175±5
Rubber no. 1	0.0868	0.0075	34±1	only).	65±5	52±28	85±17	27±2	90±10	62±35	115±15	25±15	323±3	287±8
at 20°C	0.1156	0.0134	51±1	35	80±10	77±32	132±22	70±0	167±12	115±45	215±15	102±2	435±0	390±0
The mean results	0.1445	0.0208	95±0	80	135±25	135±0	200±30	130±10	258±18	190±50	335±32	215±10	550±0	501±1
for the two	0.1735	0.0300	150±5	135	240±5	192±2	280±35	157±7	375±35	300±50	490±30	360±20	652±7	610±0
directions of twist	0.2025	0.0408	227±2	200	340±20	267±2	380±30	290±5	520±40	438±48	705±5	550±20	755±5	702±10
are given.	0.2310	0.0534	308±8	280	447±2	377±2	515±25	400±0	670±35	592±37	850±40	765±15	852±6	820±5
	0.2600	0.0676	420±5	370	570±0	515±5	630±20	555±5	880±20	780±40	1160±30	1030±30	950±15	913±13
	0.2890	0.0837	510±0	500	730±0	645±30	855±5	745±5	1105±15	977±7	1460±40	1350±40	1052±18	1018±18
	0.3180	0.1015	610±0	607	902±2	850±0	1040±0	965±5	1355±5	1272±25	1760±40	1705±55	1145±20	1137±3
	0.3470	0.1206	760±0		1070±0		1272±22		1655±5		2135±45		1232±28	
	0.0289	0.0008			20		35		10				125	96
	0.0579	0.0033			40	30	70	45	50	30	80	50	250	205
	0.0868	0.0075	5		60	50	120	90	125	90	175	150	372	338
rubber no. 2	0.1158	0.0134	50	10	115	90	205	180	210	190	300	260	495	465
at 19°C	0.1445	0.0208	150	95	170	130	280	260	345	300	430	400	607	588
	0.1735	0.0300	235	185	290	205	420	370	500	420	640	580	720	703
	0.2025	0.0408	335	275	370	320	520	490	660	610	870	800	835	825
	0.2310	0.0534	400	390	500	475	670	650	850	830	1080	1060	950	918
	0.2600	0.0676	520		640		850		1100		1380		1045	

Table 1 continued

Sample	ψ rad. cm^{-1}	ψ^2 rad^2.cm^{-2}	N(gms) at A		N(gms) at B		N(gms) at C		N(gms) at D		N(gms) at E		Torque (kg. cm)	
			increasing strain	decreasing strain	inc. strain	dec. strain	incr. strain	decr. strain	incr. strain	decr. strain	incr. strain	decr. strain	incr. strain	decr. strain
	0.0289	0.0008	20		40		30		15		30		147	107
	0.0579	0.0033	40		65		80		50		110	20	305	285
	0.0868	0.0075	50	30	110		160	40	110		210	70	470	410
	0.1158	0.0134	80	45	160	30	220	70	180	20	340	175	625	590
rubber no. 3	0.1445	0.0208	100	85	200	110	310	190	290	150	515	350	770	700
at 19°C	0.1735	0.0300	200	180	310	205	470	340	460	320	765	600	925	875
	0.2025	0.0408	270	240	445	340	600	500	660	570	1000	975	1060	970
	0.2310	0.0534	355	355	590	540	765	710	870	780	1300	1290	1180	1170
	0.2600	0.0676	470		815		1000		1140		1760		1310	
	0.0289	0.0008					10		15		20		100	65
	0.0579	0.0033					35		45		50		165	157
	0.0868	0.0075	25				70		90		110	5	265	230
rubber no. 4	0.1158	0.0134	30	25	102		100	20	145	10	200	80	330	325
at 18°C	0.1445	0.0208	70	50	140	95	180	90	200	80	300	180	425	392
	0.1735	0.0300	100	90	170	155	255	180	280	175	440	320	490	485
	0.2025	0.0408	145	115	285	220	350	285	395	305	603	525	560	560
	0.2310	0.0534	155	135	345	315	465	400	545	475	800	710	655	640
	0.2600	0.0676	255	240	450	425	605	555	700	660	1050	980	720	700
	0.2890	0.0837	305		575		760		905		1310		795	
	0.0289	0.0008	5				20				40		107	90
	0.0579	0.0033	10		35		50		70		80		195	185
	0.0868	0.0075	25		75	10	100		110		150		310	287
	0.1158	0.0134	65		125	50	150	40	160		230	80	412	385
rubber no. 5	0.1445	0.0208	100	35	175	110	220	100	230	70	310	180	500	490
at 20°C	0.1735	0.0300	150	70	245	185	310	200	320	170	440	315	605	575
	0.2025	0.0408	210	160	315	280	400	320	470	350	580	520	692	690
	0.2310	0.0534	290	265	405	385	500	475	640	620	770	730	787	770
	0.2600	0.0676	380		520		690		850		1000		875	

Table 2 The variation of normal load with ψ at various radial positions over the end plates of the parallel plate samples. All loads measured after ten minutes at each strain increment

Sample	ψ rad. cm^{-1}	ψ^2 rad.^{2} cm^{-2}	N(gms) at A		N(gms) at B		N(gms) at C		N (gms) at D		N (gms) at E		Torque (kg. cms)	
			increasing strain	decreasing strain	inc. strain	dec. strain	inc. strain	dec. strain	inc. strain	dec. strain	inc. strain	dec. strain	inc. strain	dec. strain
	0.0289	0.0008			25		25	50	5		25	25	120	75
	0.0579	0.0033			45	45	60	60	60	55	85	60	242	190
	0.0868	0.0075	10	5	75	75	115	120	130	120	170	135	367	310
rubber no.2	0.1158	0.0134	50	20	115	115	200	195	230	220	300	250	490	435
at 19°C	0.1445	0.0208	80	45	180	170	285	265	360	345	450	400	580	555
	0.1735	0.0300	225	180	320	280	400	390	520	490	660	585	685	677
	0.2025	0.0408	345	290	380	350	545	500	690	625	875	780	815	792
	0.2310	0.0534	405	380	555	525	690	680	910	870	1100	1060	922	917
	0.2600	0.0676	620		690		900		1160		1390		1007	
	0.0289	0.0008	20		25		10		10		20		155	95
	0.0579	0.0033	30		70		50		50		70		307	235
	0.0868	0.0075	45	50	120	30	130	50	110		170	50	465	390
rubber no.3	0.1158	0.0134	60	60	155	86	190	130	180	70	270	170	615	560
at 19°C	0.1445	0.0208	80	80	200	145	290	245	260	190	450	390	755	697
	0.1735	0.0300	180	170	290	240	420	370	420	340	700	610	905	867
	0.2025	0.0408	250	225	420	370	585	520	620	525	970	880	1052	1012
	0.2310	0.0534	340	300	575	540	760	710	820	760	1280	1215	1172	1167
	0.2600	0.0676	470		785		985		1090		1680		1320	
	0.0289	0.0008					5		15		35		85	55
	0.0579	0.0033			15	5	15		35		45		162	135
	0.0868	0.0075			35	15	40		80	20	110		252	230
rubber no.4	0.1158	0.0134	30	15	55	35	75	15	130	80	180	80	332	317
at 18°C	0.1445	0.0208	65	40	105	75	110	60	200	190	270	170	407	385
	0.1735	0.0300	100	90	170	125	180	120	290	230	405	300	480	467
	0.2025	0.0408	140	130	240	200	265	220	415	365	570	495	562	540
	0.2310	0.0534	185	170	330	300	375	335	550	510	760	705	627	620
	0.2600	0.0676	240	225	455	415	500	470	720	690	1010	960	707	707
	0.2890	0.0837	290		575		640		925		1280		790	

Table 2 continued.

Sample	ψ rad. cm^{-1}	ψ^2 rad.^{2} cm^{-2}	N(gms) at A		N(gms) at B		N(gms) at C		N(gms) at D		N(gms) at E		Torque (kg. cms)	
			increasing strain	decreasing strain	incr. strain	decr. strain	incr. strain	decr. strain	incr. strain	decr. strain	incr. strain	decr. strain	incr. strain	decr. strain
	0.0289	0.0008	5		10		15		40		50		105	72
	0.0579	0.0033	15		35		40		70		100		190	170
	0.0868	0.0075	30		75	5	90		110		170	30	310	277
	0.1158	0.0134	45		120	50	145	40	180	80	250	110	397	375
sample no. 5 at 20°C	0.1445	0.0208	105	65	160	100	210	120	240	140	340	220	512	483
	0.1735	0.0300	170	135	230	170	290	205	320	205	450	340	592	583
	0.2025	0.0408	240	155	305	260	390	340	480	360	590	520	690	685
	0.2310	0.0534	310	240	395	365	510	510	650	640	770	760	780	780
	0.2600	0.0676	385		510		690		850		1000		875	
							20	30	5	30	10	75	94	62
	0.0349	0.0012	20				35	60	40	60	45	100	190	156
	0.0698	0.0049	30		10		80	115	85	105	105	160	289	250
	0.1047	0.0109	45	80	35	50	135	160	150	165	210	250	375	344
sample no. 7	0.1395	0.0195	75	90	70	85	200	220	240	245	330	360	458	430
at 25°C	0.1745	0.0303	110	115	135	135	295	295	340	350	500	500	537	503
	0.2090	0.0438	160	165	220	240	415	405	470	470	680	770	620	594
	0.2440	0.0595	210	215	315	305	545		620		890		687	
	0.2790	0.0779	275		410									

Time (minutes)	t_{zz} ($g.cm^{-2}$) at holes A to E					Torque (kg-cms)	
	A	B	C	D	E	(A,D)	(B,C,E)
1	496		785			375	384
2		641		863			376
3					977		
4	465		749				375
5				810	883	361	372
7	459				863		362
8		573		795			362
9					852		
10	450		730			350	359
11		563		785			356
12					836		
13	447		731				350
14		552		775			350
17		549	712				348
18				761			
19							338
20	443		706			338	334
21		542			823		332
23				759			
26	435						
28		533					326
30			690				
31				747	818	320	326
32		530					
35	425						
36				739			
40		521	689				
43	421					312	
44				731			
45			680				
46		520					
52					804		
55	415						
56				715			
61		514	678				332
65					803		
68	411					317	
69				716			
79					803		
82		504	678				336
85				706		312	
88	414						

Table 4. Normal stress relaxation at the five holes in the end plate of rubber No. 6. Torque relaxation was determined for the 2 samples needed to complete normal stress measurements.

Time (minutes)	t_{zz} (g.cm^{-2}) at holes A to E					Torque (kg-cms)	
	A	B	C	D	E	(A,D)	(B.C.E)
91					797		
97	405					314	
98				700			
110					796		
116	402					312	
117				697			
120					795		
135				690		300	
137	406						
142		486	630				306
170					780		
182	378			676		306	
225		471	602				290
247	366			655		300	
259					747		
356	329			628		301	
370		455	585				303
372					732		
805		451	543		642		294
1106	302			461			
1166	320			482			
1455		323	451		494		

Table 4 (continued)

Rubber No.	Increasing strains ($\Psi a = 1.3$) decreasing strains ($\Psi a = 1.0$)							
	2 minute time interval		10 minute time interval		2 minute time interval		10 minute time interval	
	$\frac{\partial W}{\partial I_2}$	A	$\frac{\partial W}{\partial I_2}$	A	$\frac{\partial W}{\partial I_2}$	A	$\frac{\partial W}{\partial I_2}$	A
1	125±5	1300			100±35	1000		
2	125±30	1580	135±30	1570	65±35	1375	75±15	1380
3	130±35	1925	135±30	1860	105±5	1770	115±15	1650
4	75±25	1170	65±25	1125	50±25	930	55±15	910
5	120±0	1125	100±20	1110	80±25	945	95±15	940
7			65±10	735			60±10	910

Table 5. A and $\frac{\partial W}{\partial I_2}$ ($g.cm^{-2}$), determined from the normal stress on the axis and at the edge respectively. The stress at the edge was found by a straight line extrapolation of the normal stress distribution.

Rubber No.	Increasing strains ($\Psi a = 1.3$) decreasing strains ($\Psi a = 1.0$)							
	2 minute time interval		10 minute time interval		2 minute time interval		10 minute time interval	
	C_2	C_1	C_2	C_1	C_2	C_1	C_2	C_1
1	47	1277			33	977		
2	52	1544	68	1581	19	1363	41	1406
3	-42	1856	-9	1767	-42	1646	-40	1572
4	-38	1124	-35	1070	-28	887	-41	893
5	68	1126	69	1128	28	940	49	953
7					10	839	-1	882

Table 6 The Mooney parameters C_1 and C_2, ($g.cm^{-2}$) determined from the straight lines in figures 25 to 28.

Rubber No.	N/2A ($kg.cm^{-2}$)	Increasing load λ	Increasing load $\frac{\partial W}{\partial I_1} + \frac{1}{\lambda}\frac{\partial W}{\partial I_2}$ ($kg.cm^{-2}$)	Decreasing load λ	Decreasing load $\frac{\partial W}{\partial I_1} + \frac{1}{\lambda}\frac{\partial W}{\partial I_2}$ ($kg.cm^{-2}$)
	1.10	1.158	2.69	1.115	2.35
	1.47	1.226	2.62	1.260	2.33
	1.84	1.299	2.60	1.340	2.35
	2.21	1.390	2.54	1.420	2.39
	2.50	1.480	2.51	1.514	2.39
1	2.94	1.591	2.46	1.632	2.34
	3.31	1.705	2.43	1.732	2.37
	3.68	1.842	2.38	1.886	2.29
	4.05	1.985	2.33	2.033	2.26
	4.41	2.140	2.30	2.158	2.26
	4.78	2.270	2.30		
	1.14	1.130	3.17	1.105	1.97
	1.52	1.190	3.13	1.205	2.47
	1.90	1.252	3.09	1.280	2.82
	2.27	1.320	3.05	1.355	2.81
	2.66	1.400	2.98	1.442	2.77
2	3.04	1.490	2.92	1.525	2.77
	3.41	1.568	2.93	1.635	2.71
	3.79	1.683	2.85		
	4.17	1.790	2.82	1.850	2.68
	4.55	1.918	2.77		
	4.93	1.980	2.74	2.078	2.67
	6.45	2.490	2.77		
	1.07	1.110	3.58		
	1.79	1.204	3.46		
	2.14	1.259	3.41	1.281	3.19
	2.86	1.374	3.39	1.401	3.21
3	3.22	1.452	3.29	1.472	3.19
	3.57	1.534	3.22		
	3.93	1.620	3.17	1.628	3.14
	4.29	1.691	3.19		
	4.65	1.780	3.17	1.800	3.11
	6.08	2.118	3.21		
	0.61	1.127	2.15	1.153	1.52
	0.98	1.222	1.96	1.254	1.59
	1.22	1.295	1.875	1.332	1.59
	1.47	1.382	1.835	1.420	1.59
	1.96	1.583	1.72	1.636	1.55
4	2.45	1.833	1.65	1.898	1.515
	2.94	2.080	1.635	2.200	1.475
	3.43	2.330	1.625	2.470	1.485
	3.92	2.569	1.66	2.691	1.54
	4.41	2.780	1.70	2.850	1.62
	4.90	2.965	1.75		

Table 10 Simple extension data. The load N is applied to samples of unstrained cross-sectional area A.

Table 10 (continued)

Rubber No.	N/2A ($kg.cm^{-2}$)	Increasing load λ	Increasing load $\frac{\partial W}{\partial I_1} + \frac{1}{\lambda}\frac{\partial W}{\partial I_2}$ ($kg.cm^{-2}$)	Decreasing load λ	Decreasing load $\frac{\partial W}{\partial I_1} + \frac{1}{\lambda}\frac{\partial W}{\partial I_2}$ ($kg.cm^{-2}$)
	0.63	1.092	2.51	1.108	2.16
	0.88	1.131	2.52		
	1.26	1.200	2.49		
	1.52	1.255	2.435	1.270	2.335
	2.02	1.369	2.42	1.392	2.31
5	2.53	1.505	2.37	1.535	2.28
	3.03	1.662	2.33	1.695	2.255
	3.53	1.845	2.28	1.875	2.23
	4.04	2.040	2.245	2.070	2.20
	5.05	2.410	2.26	2.462	2.20
	6.06	2.760	2.31	2.795	2.28
	7.07	3.040	2.37		

Table 11 $\frac{\partial W}{\partial I_1}$ and $\frac{\partial W}{\partial I_2}$ from the simple extension measurements

Rubber No.	$\frac{\partial W}{\partial I_1}$ ($kg.cm^{-2}$)	$\frac{\partial W}{\partial I_2}$ ($kg.cm^{-2}$)
1	1.83	0.98
2	2.18	1.12
3	2.24	1.52
4	1.23	0.66
5	1.93	0.64

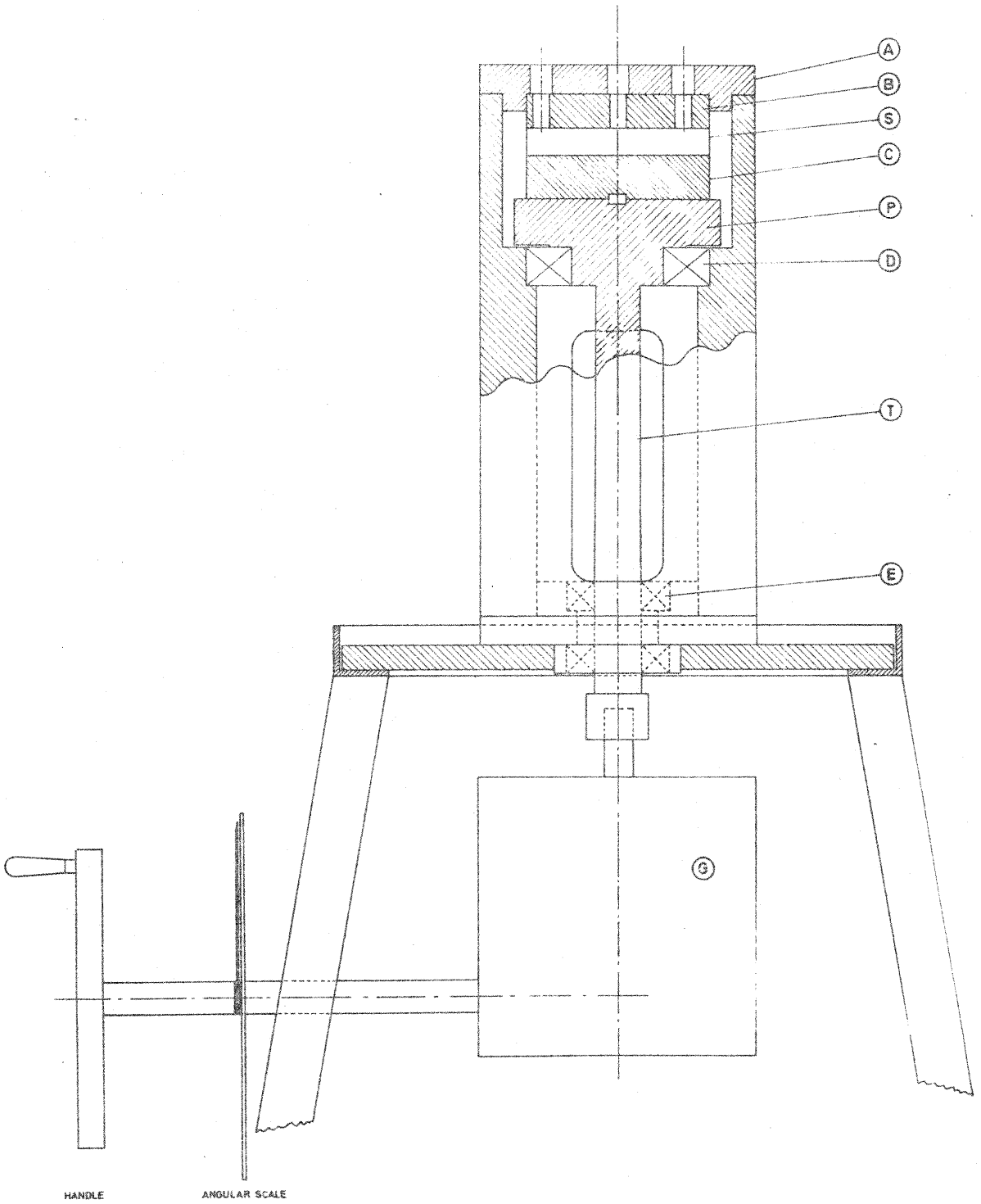

FIGURE 1 THE TORSION JIG AND SAMPLE

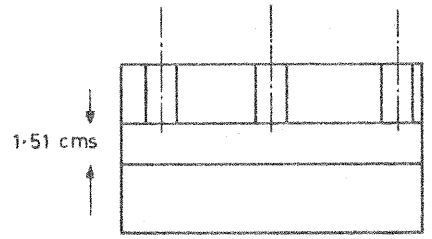

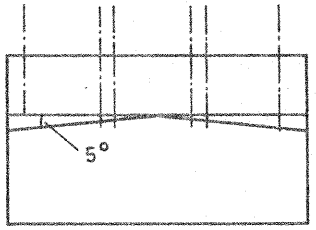

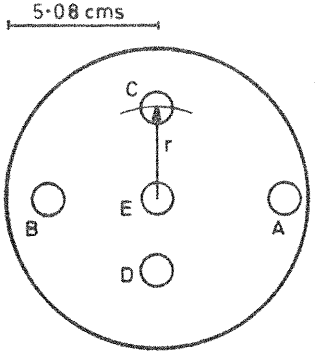

HOLE	r (cms)
A	4·31
B	3·68
C	3·05
D	2·47
E	0
1	4·5
2	4·1
3	3·8
4	3·3
5	2·8
6	2·2

HOLE DIAS. 0·95cms

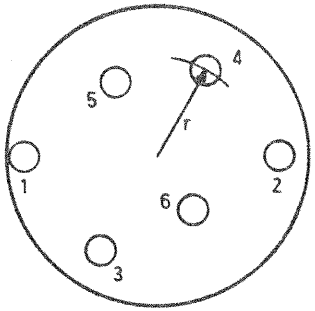

THE PARALLEL PLATE SAMPLE

THE CONE AND PLATE SAMPLE

FIGURE 2

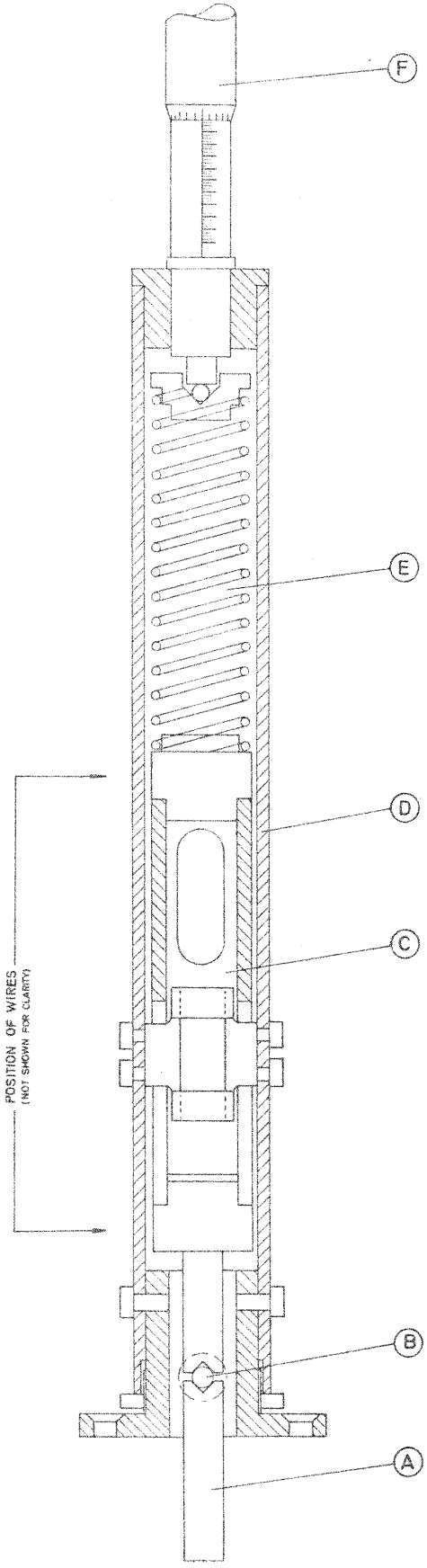

FIGURE 3
A NORMAL LOAD DYNAMOMETER

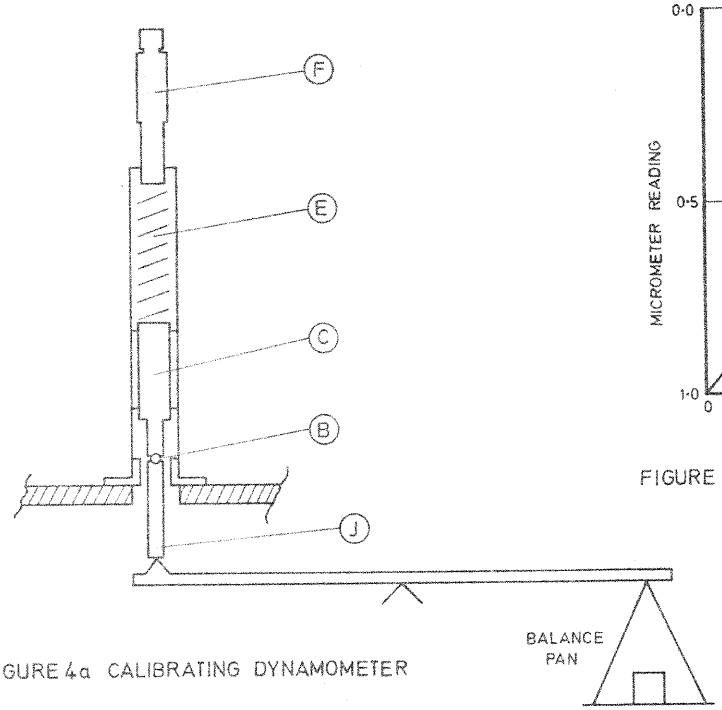

FIGURE 4a CALIBRATING DYNAMOMETER

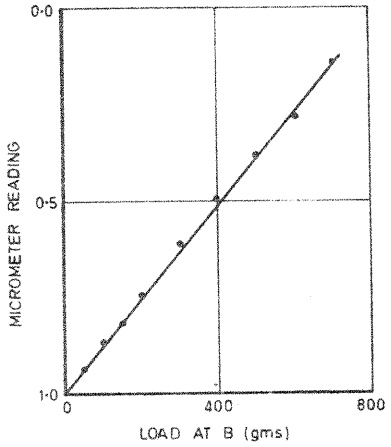

FIGURE 4b A TYPICAL DYNAMOMETER CALIBRATION

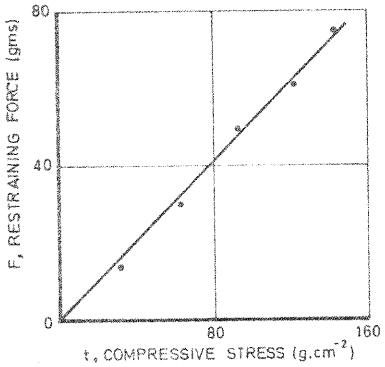

FIGURE 4c NORMAL FORCES IN PURE COMPRESSION

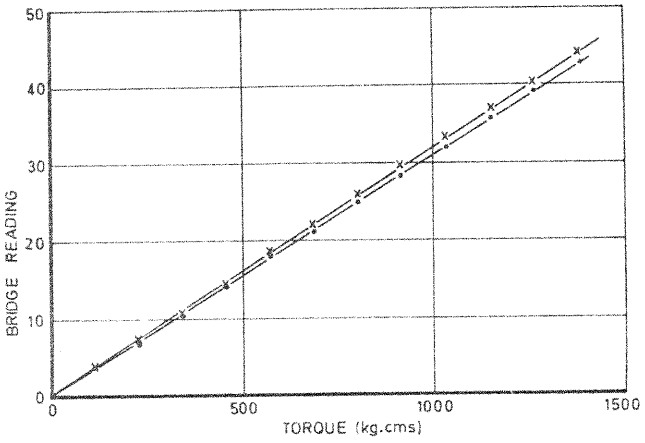

FIG. 4d THE TORQUE TUBE CALIBRATION

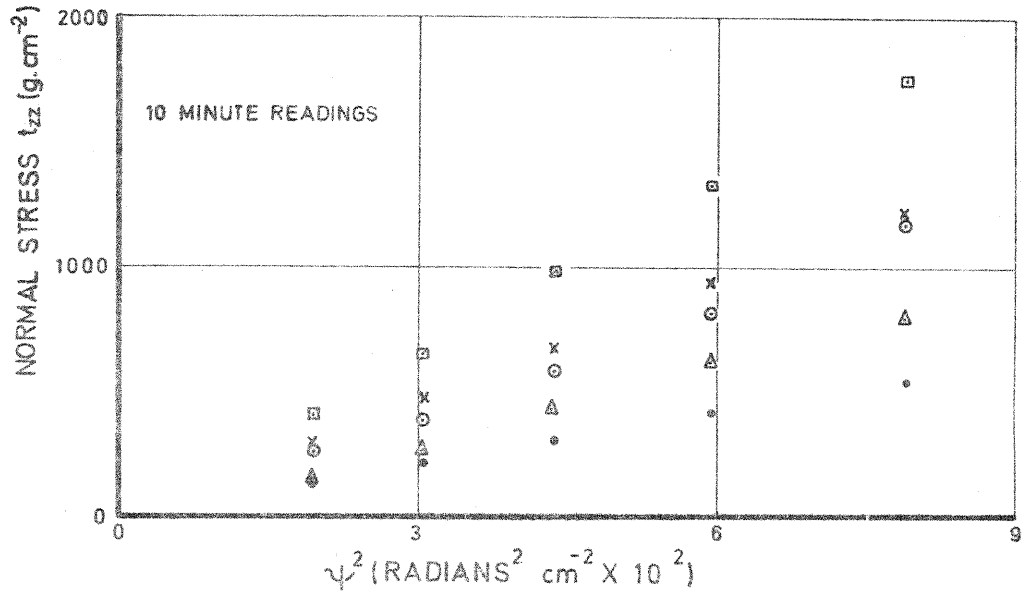

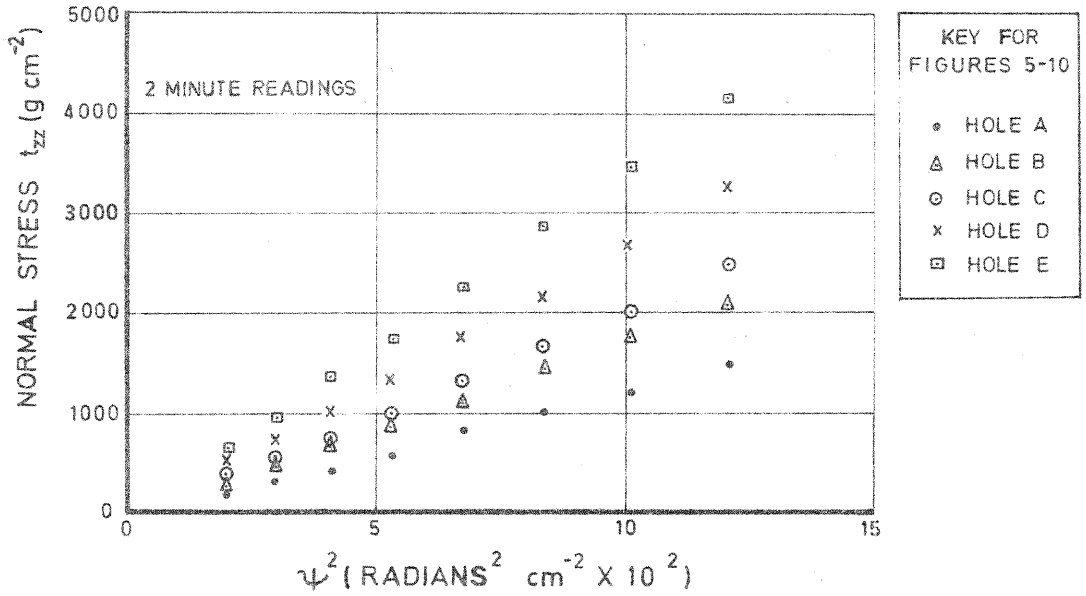

FIGURE 5 NORMAL STRESS AS A FUNCTION OF ψ^2 FOR RUBBER No.7

FIGURE 6 NORMAL STRESS AS A FUNCTION OF ψ^2 FOR RUBBER No.1

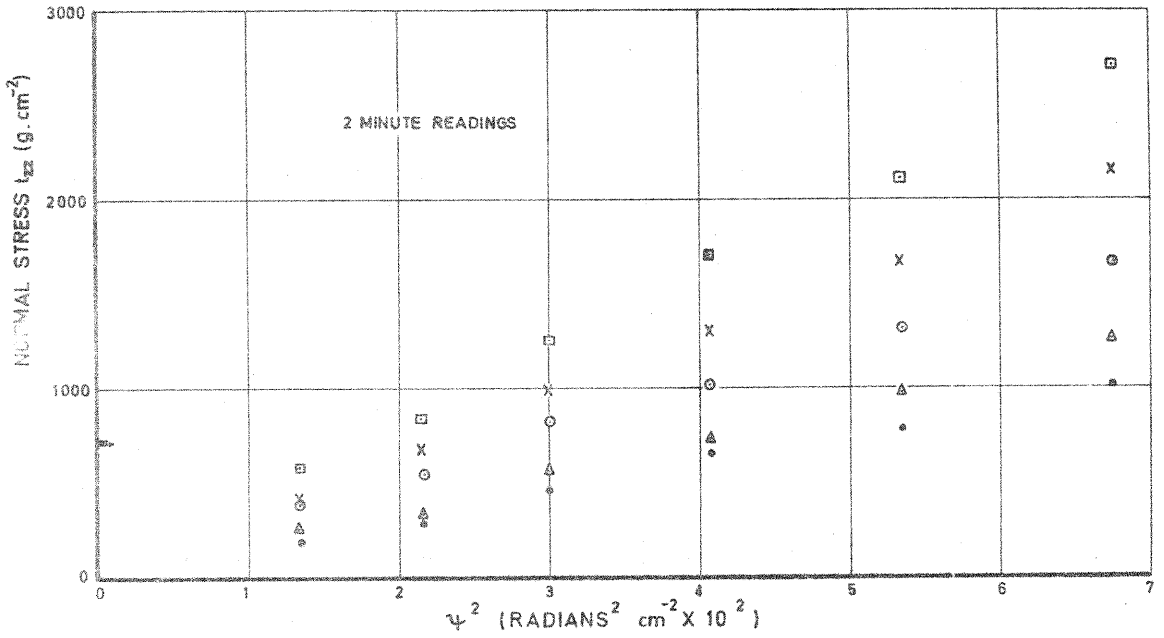

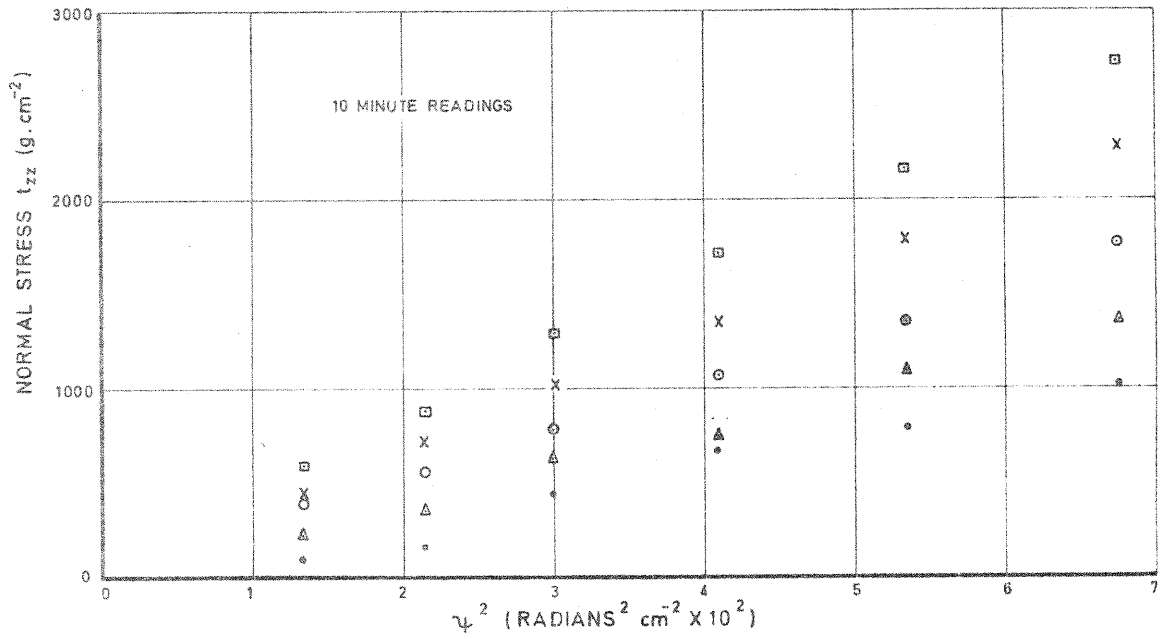

FIGURE 7. NORMAL STRESS AS A FUNCTION OF ψ^2 FOR RUBBER No. 2.

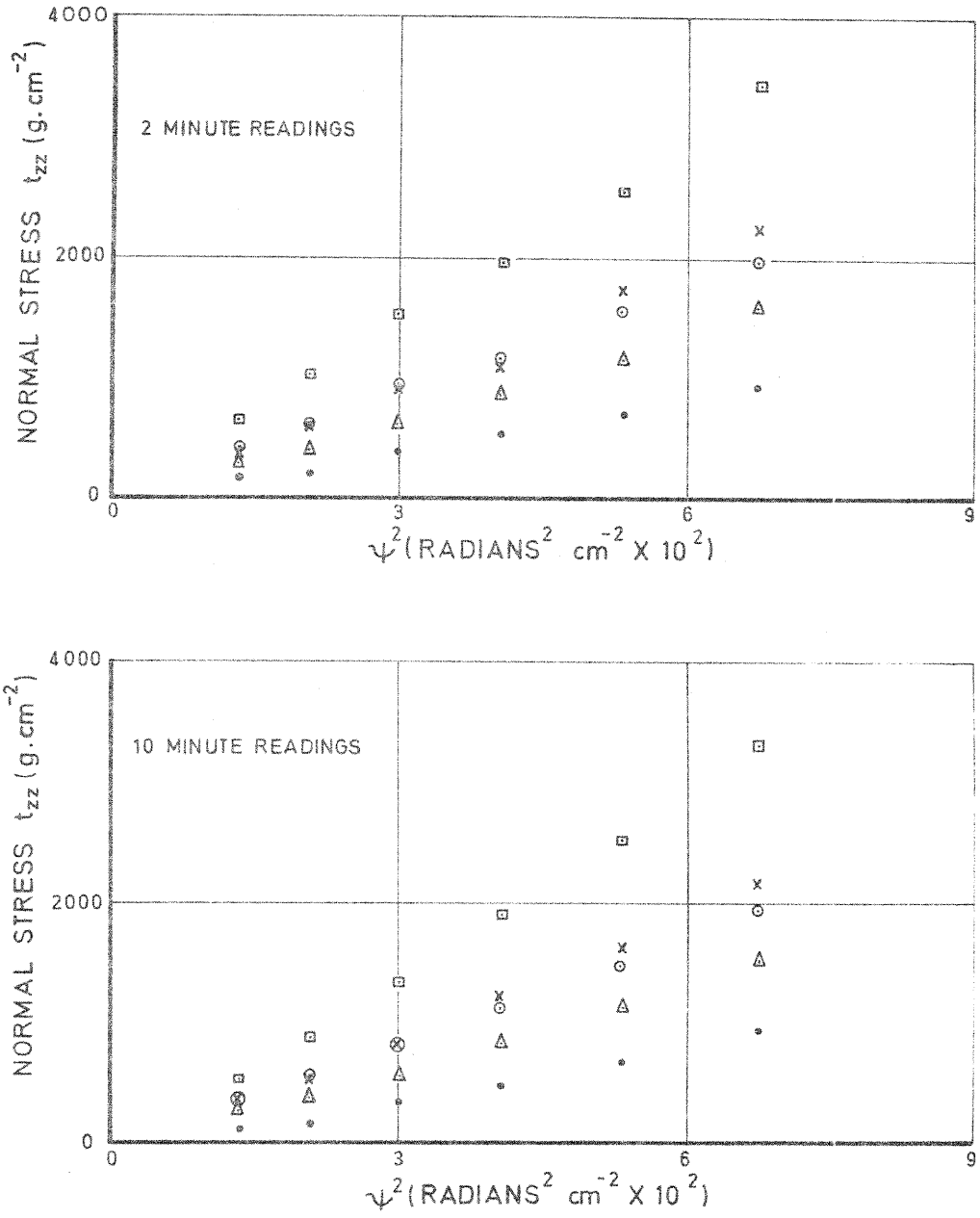

FIGURE 8 NORMAL STRESS AS A FUNCTION OF ψ^2 FOR RUBBER No. 3

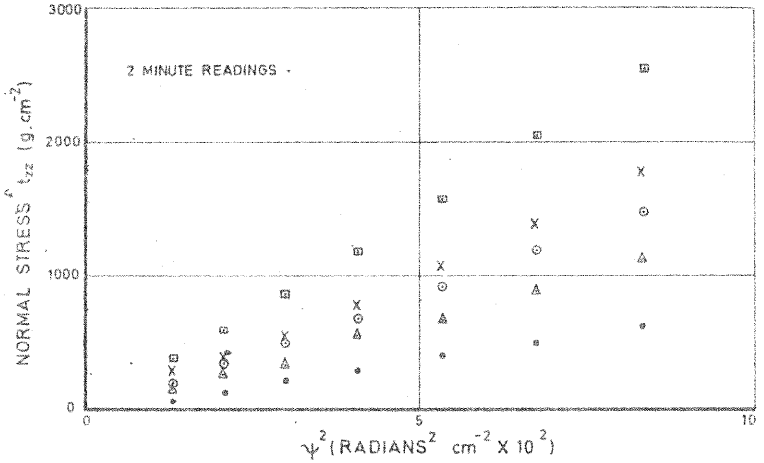

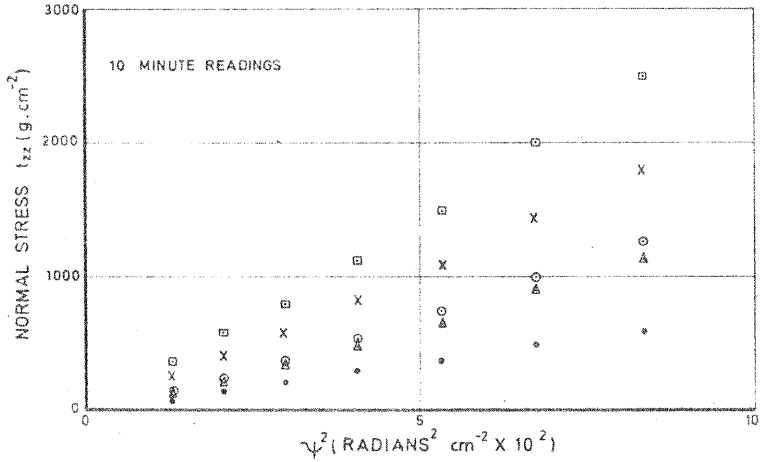

FIGURE 9 NORMAL STRESS AS A FUNCTION OF ψ^2 FOR RUBBER No. 4

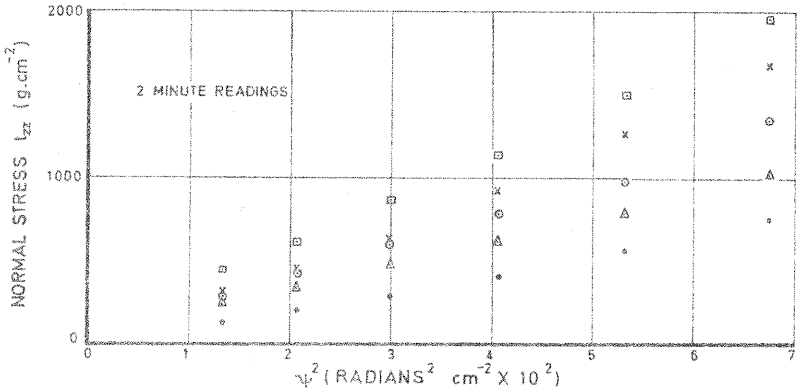

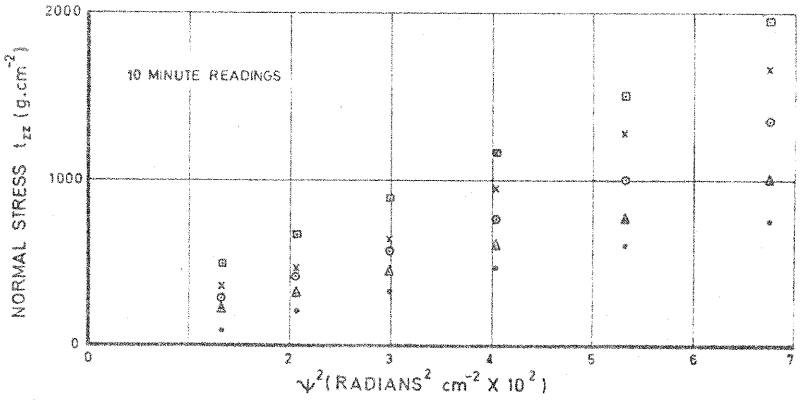

FIGURE 10 NORMAL STRESS AS A FUNCTION OF ψ^2 FOR RUBBER No. 5

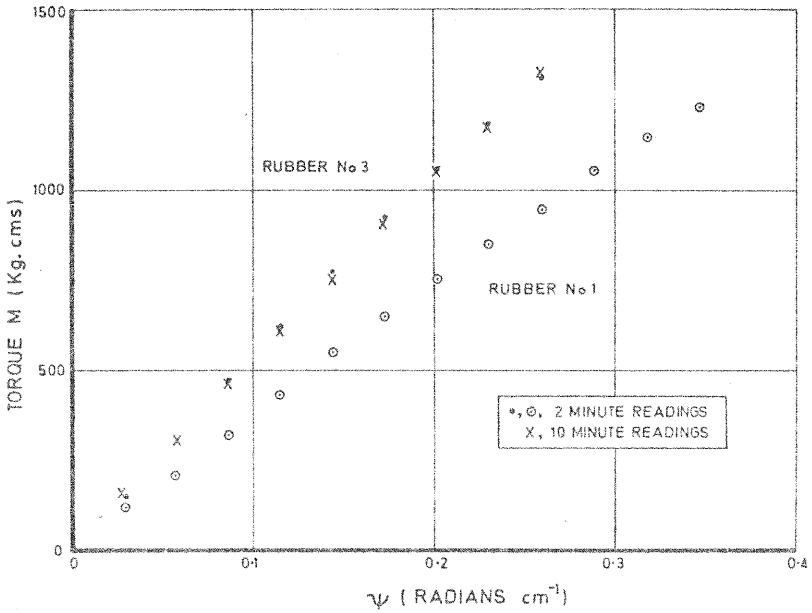

FIGURE 11 THE VARIATION OF TORQUE WITH ψ FOR RUBBER Nos. 1 and 3

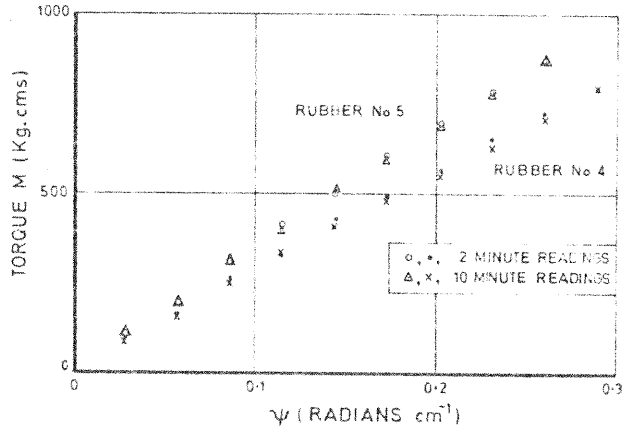

FIGURE 12 THE VARIATION OF TORQUE WITH ψ FOR RUBBER Nos. 4 and 5

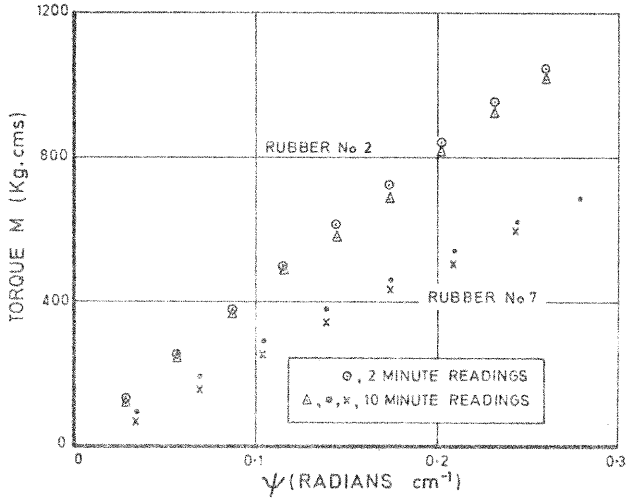

FIGURE 13 THE VARIATION OF TORQUE WITH ψ FOR RUBBER Nos. 2 and 7
THE COMPLETE DEFORMATION CYCLE IS SHOWN FOR RUBBER No. 7

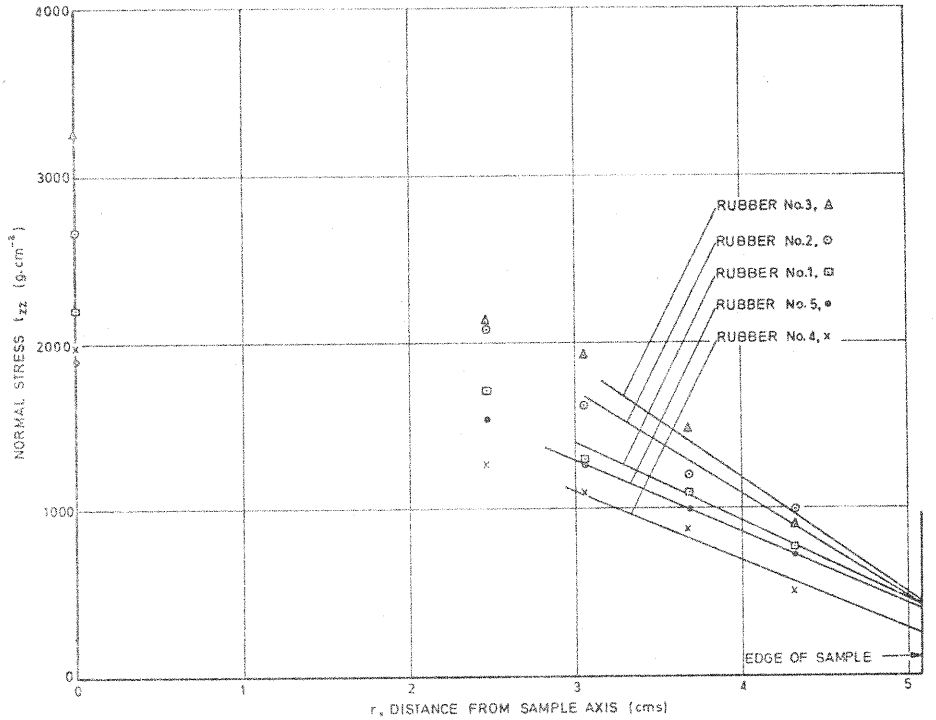

FIGURE 14. THE NORMAL STRESS DISTRIBUTION FOR INCREASING STRAIN (SURFACE SHEAR STRAIN 130%, 2 MINUTE READINGS)

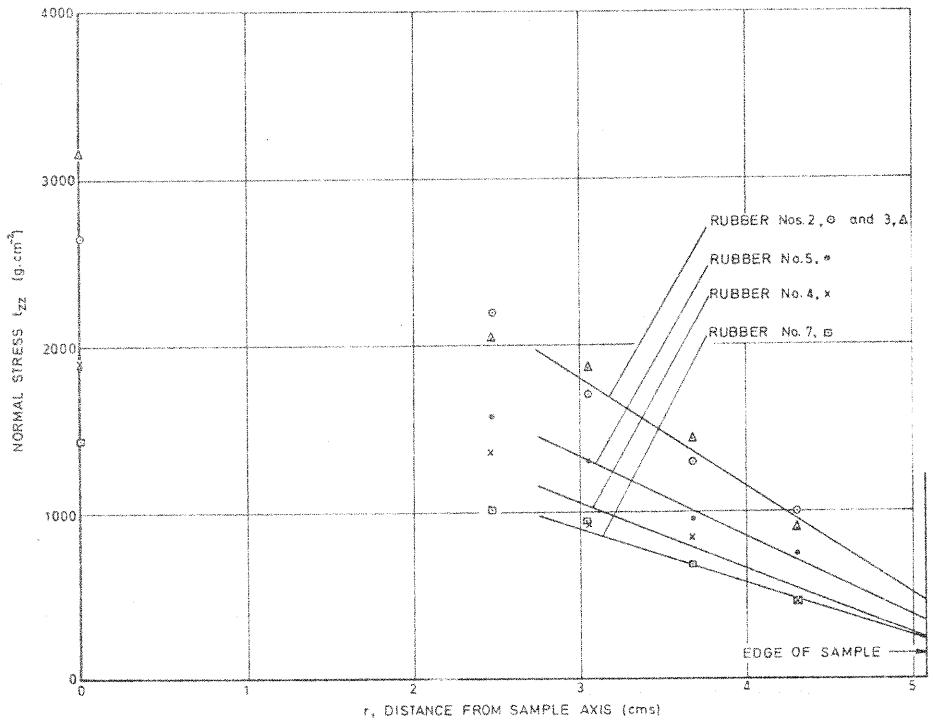

FIGURE 15. THE NORMAL STRESS DISTRIBUTION FOR INCREASING STRAIN (SURFACE SHEAR STRAIN 130%, 10 MINUTE READINGS)

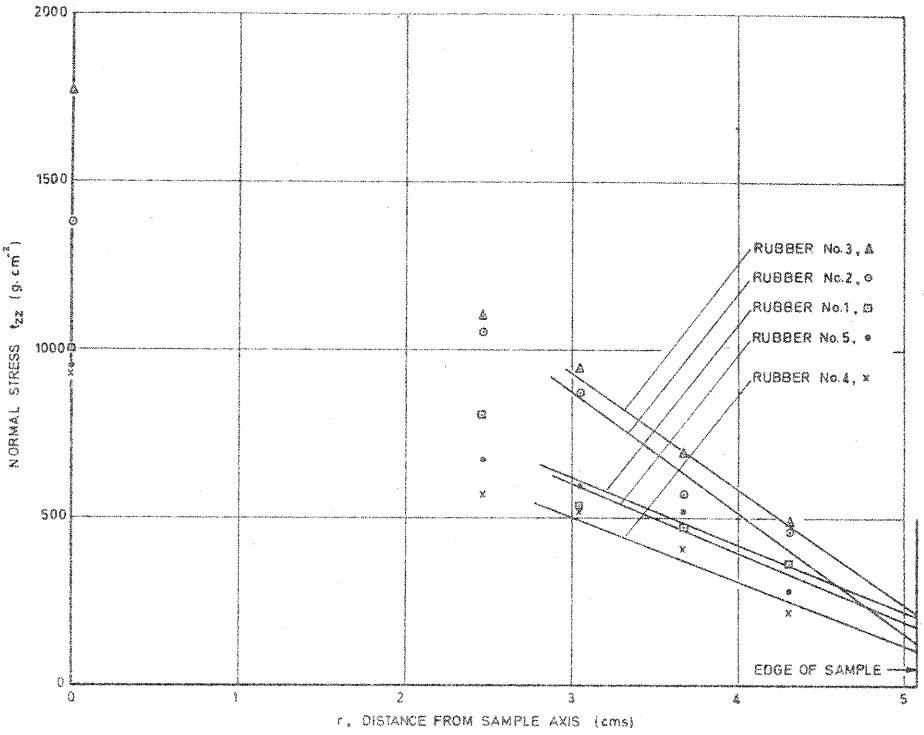

FIGURE 16. THE NORMAL STRESS DISTRIBUTION FOR DECREASING STRAIN (SURFACE SHEAR STRAIN 100%, 2 MINUTE READINGS)

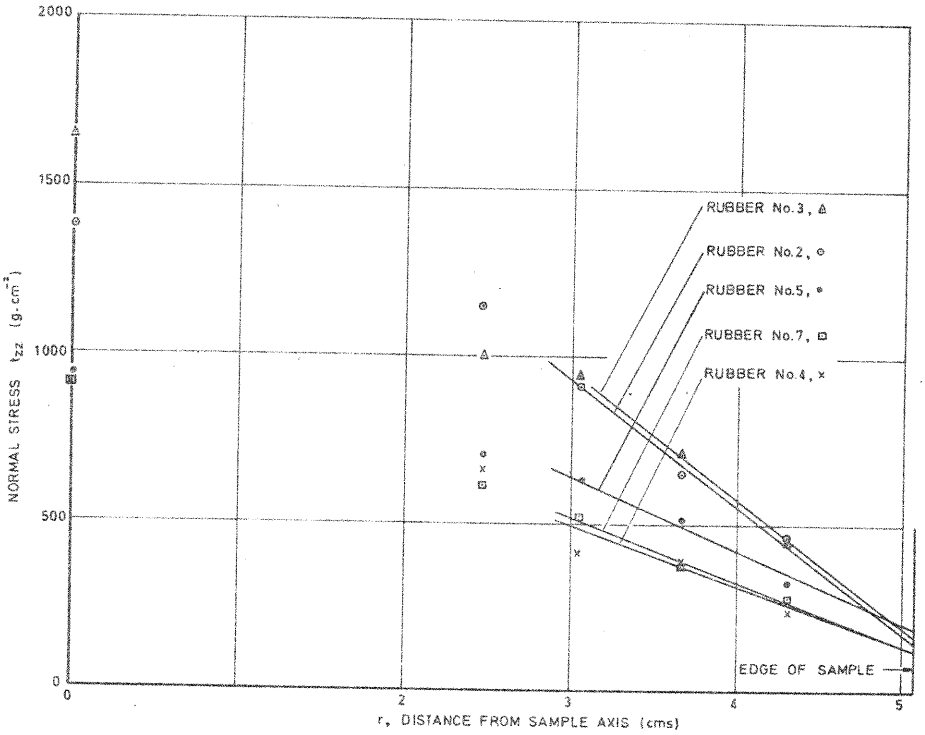

FIGURE 17. THE NORMAL STRESS DISTRIBUTION FOR DECREASING STRAIN (SURFACE SHEAR STRAIN 100 %, 10 MINUTE READINGS)

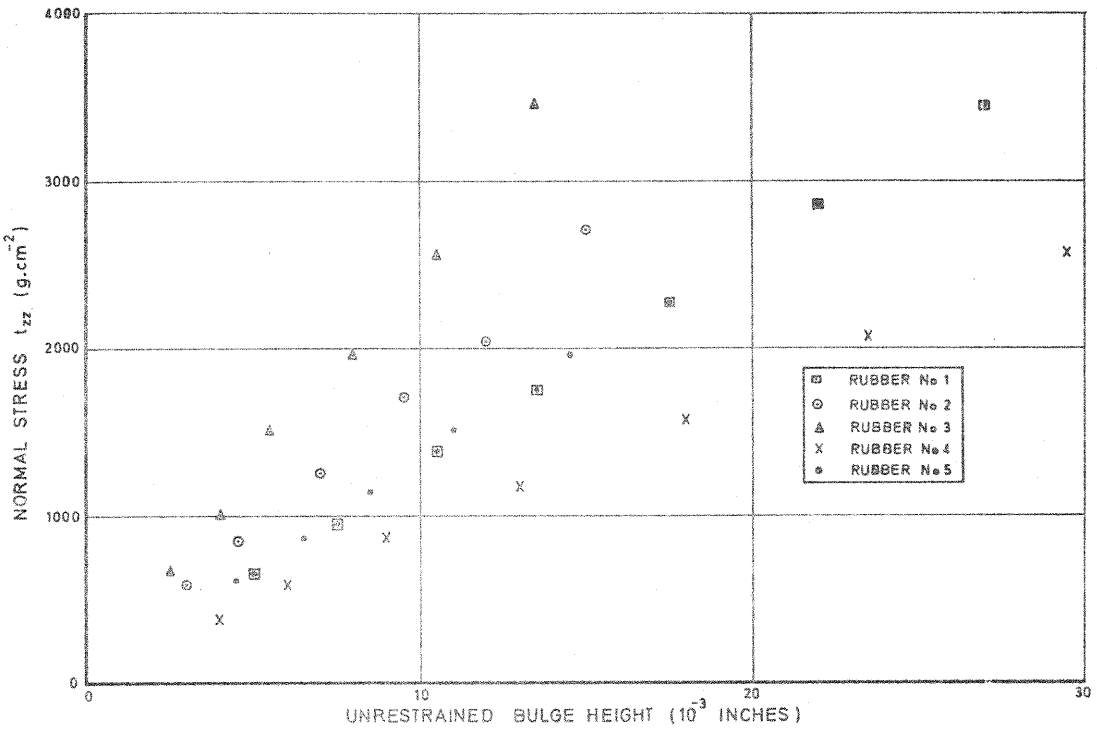

FIGURE .18. THE RELATIONSHIP BETWEEN NORMAL STRESS AND UNRESTRAINED BULGE HEIGHT. ALL MEASUREMENTS WERE MADE IN THE CENTRE HOLE OF THE END PLATE.

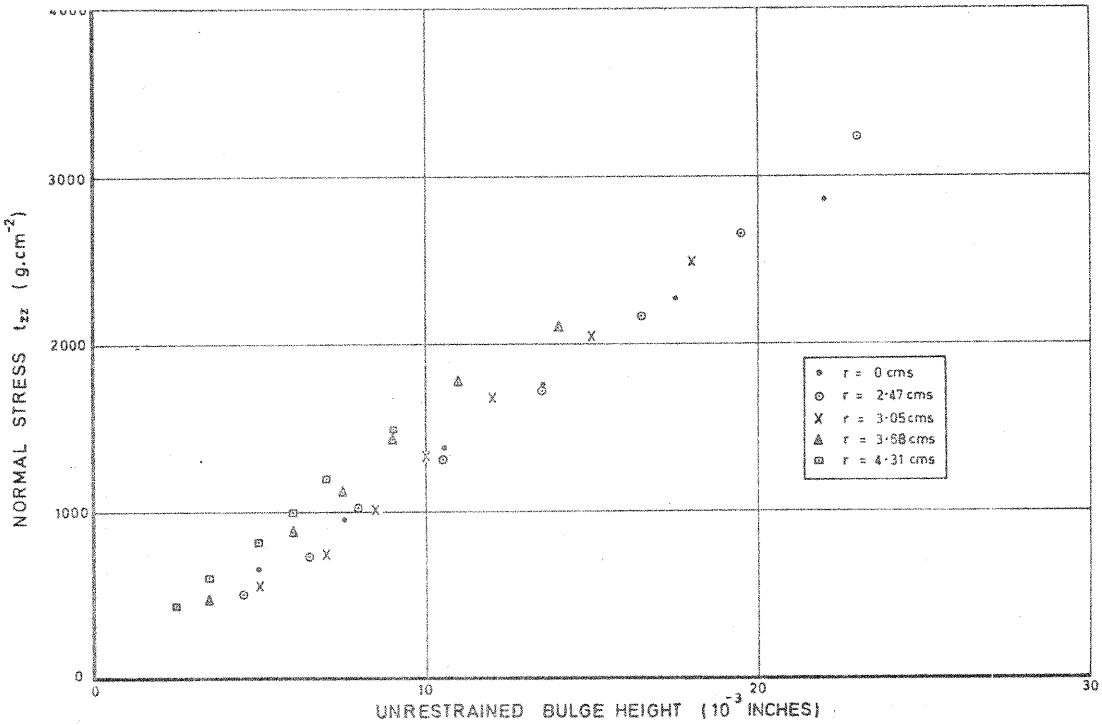

FIGURE.19. THE RELATIONSHIP BETWEEN NORMAL STRESS AND UNRESTRAINED BULGE HEIGHT FOR ALL 5 HOLES IN THE END PLATE OF RUBBER No. I.

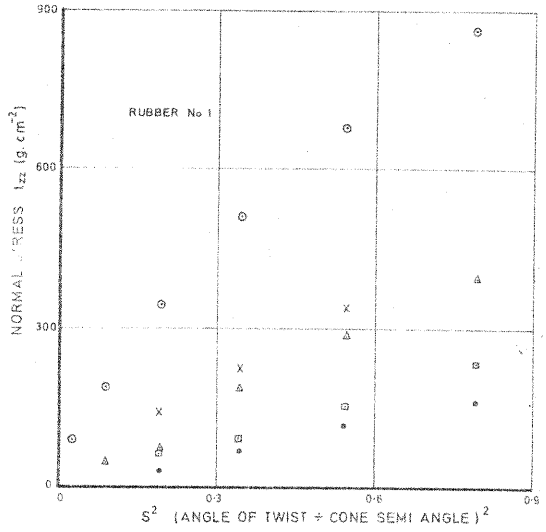

FIGURE 20 (a)

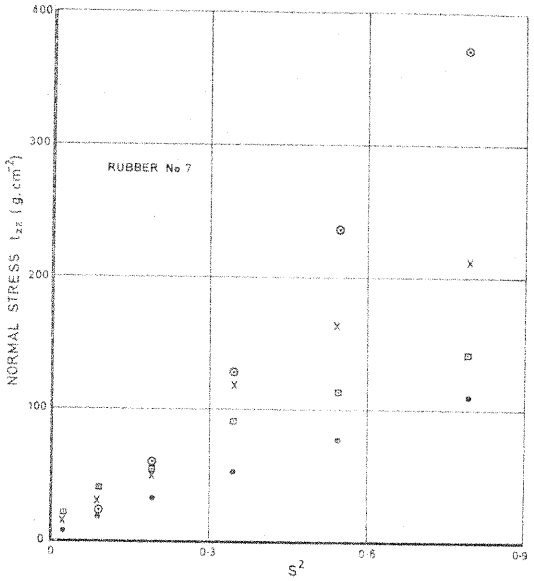

[⊙ r=2·2cms., × r=2·8cms, △ r=3·3cms., ⊡ r=3·8cms., • r=4·5cms.]

FIGURE 20 (b)

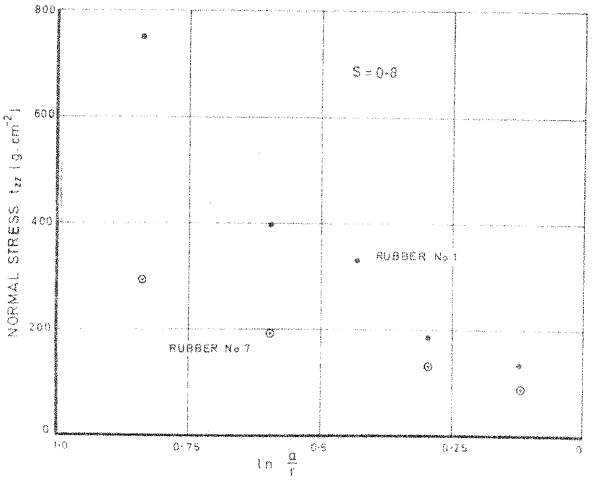

FIGURE 21

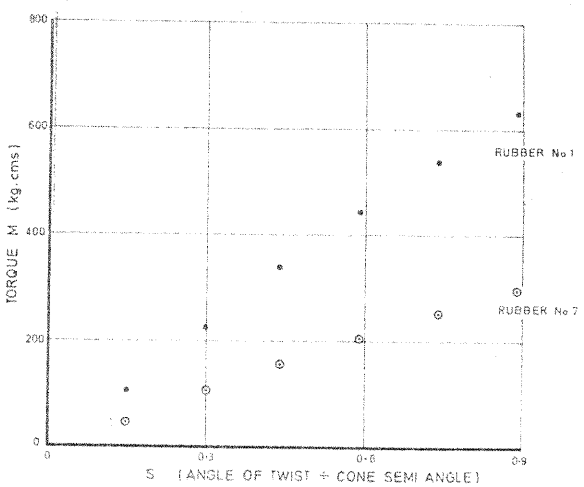

FIGURE 22

FIGURE 20 (a) and (b) THE NORMAL STRESS MEASURED ON THE CONE AND PLATE SYSTEM FOR RUBBER Nos. 1 and 7

FIGURE 21 THE NORMAL STRESS DISTRIBUTIONS IN THE CONE AND PLATE SYSTEM FOR RUBBER Nos. 1 and 7

FIGURE 22 THE TORQUE AS A FUNCTION OF S, THE RATIO OF THE ANGLE OF TWIST TO THE CONE SEMI-ANGLE

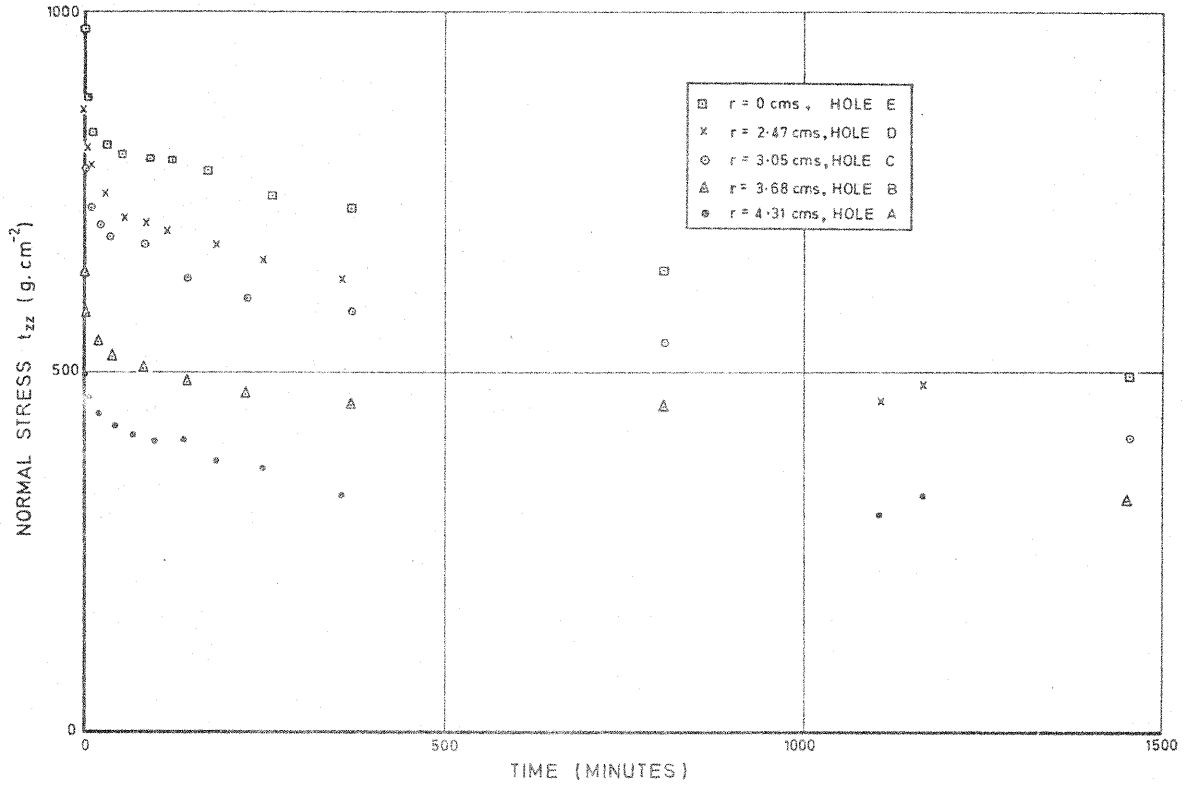

FIGURE 23 THE RELAXATION OF NORMAL STRESS FOR RUBBER No. 6 AT 132% SURFACE SHEAR STRAIN

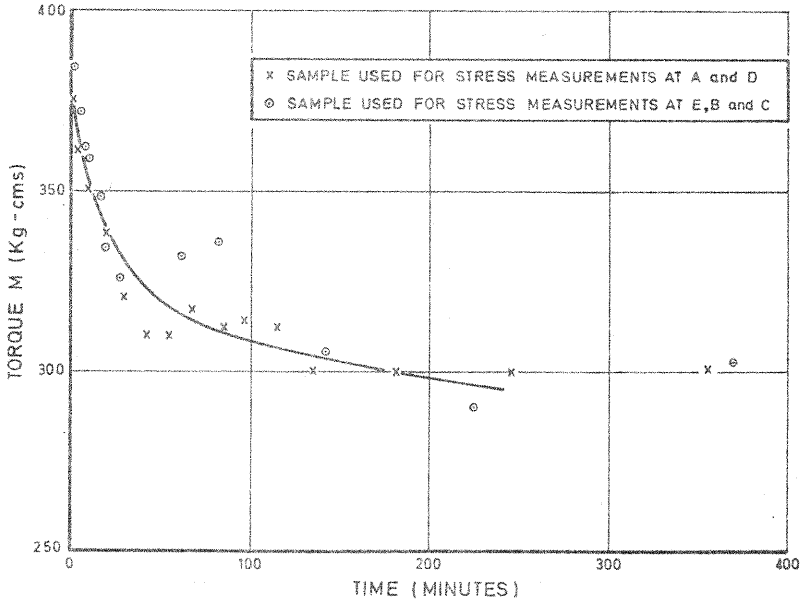

FIGURE 24 THE RELAXATION OF THE TORQUE NEEDED TO MAINTAIN A 132% SURFACE SHEAR STRAIN IN RUBBER No. 6

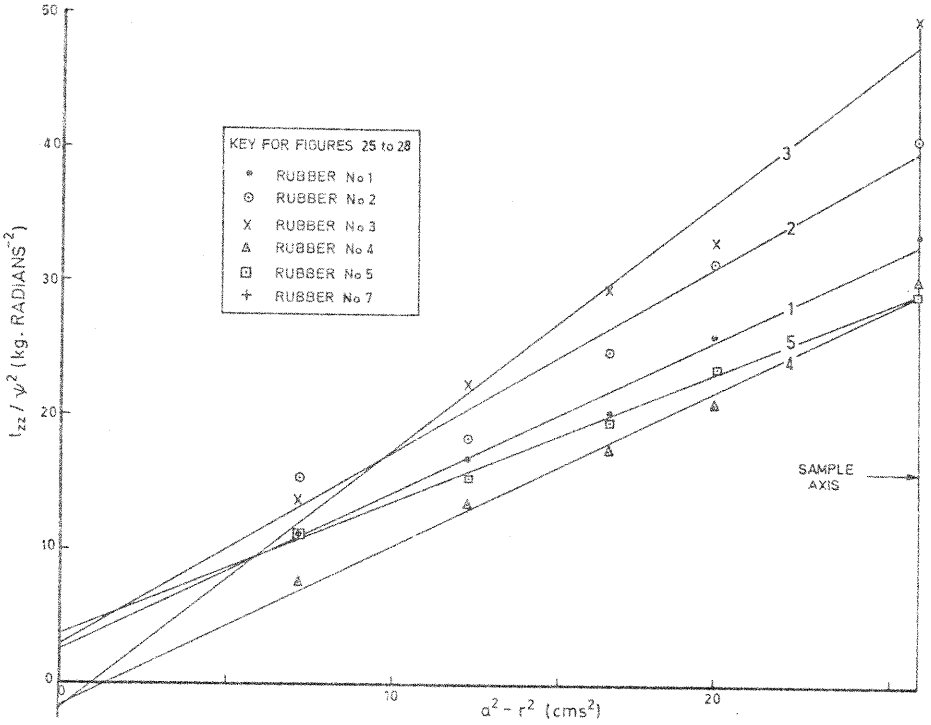

FIGURE .25.

THE EXAMINATION OF EQUATION 4.9 TO FIND C_1 AND C_2. (2 MINUTE READINGS AT $\Psi a = 1.3\ \Psi$ INCREASING). THE STRAIGHT LINES IN FIGURES 25 TO 28 WERE FOUND BY THE LEAST SQUARE METHOD. THE NUMBER INSERTED INTO EACH LINE REFERS TO THE RUBBER.

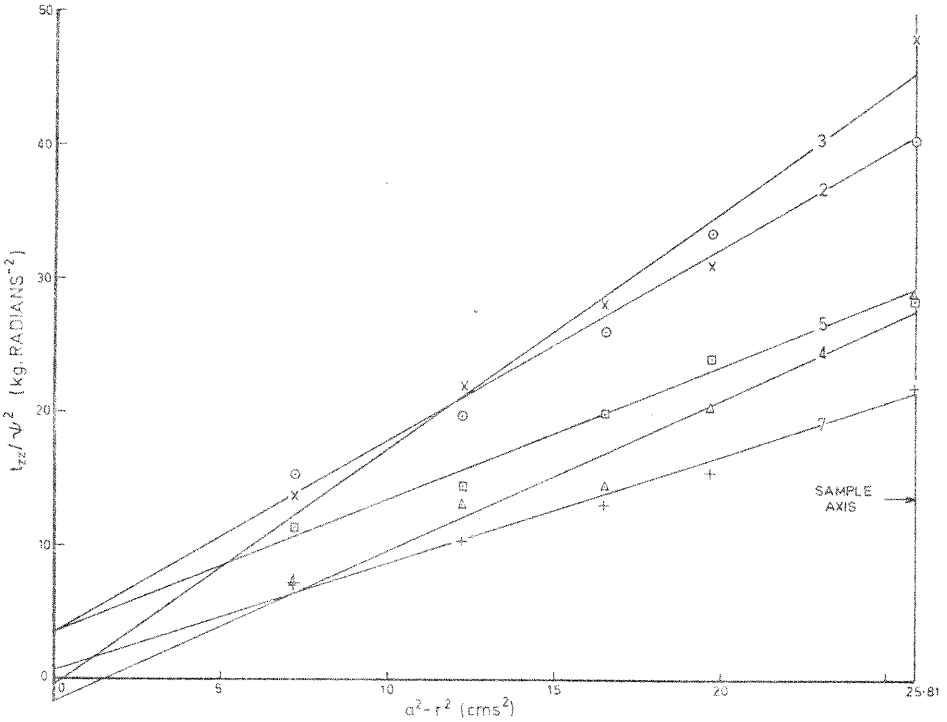

FIGURE 26 THE EXAMINATION OF EQUATION 4·9 TO FIND C_1 and C_2 (10 MINUTE READINGS AT $\psi_a = 1{\cdot}3$, ψ INCREASING)

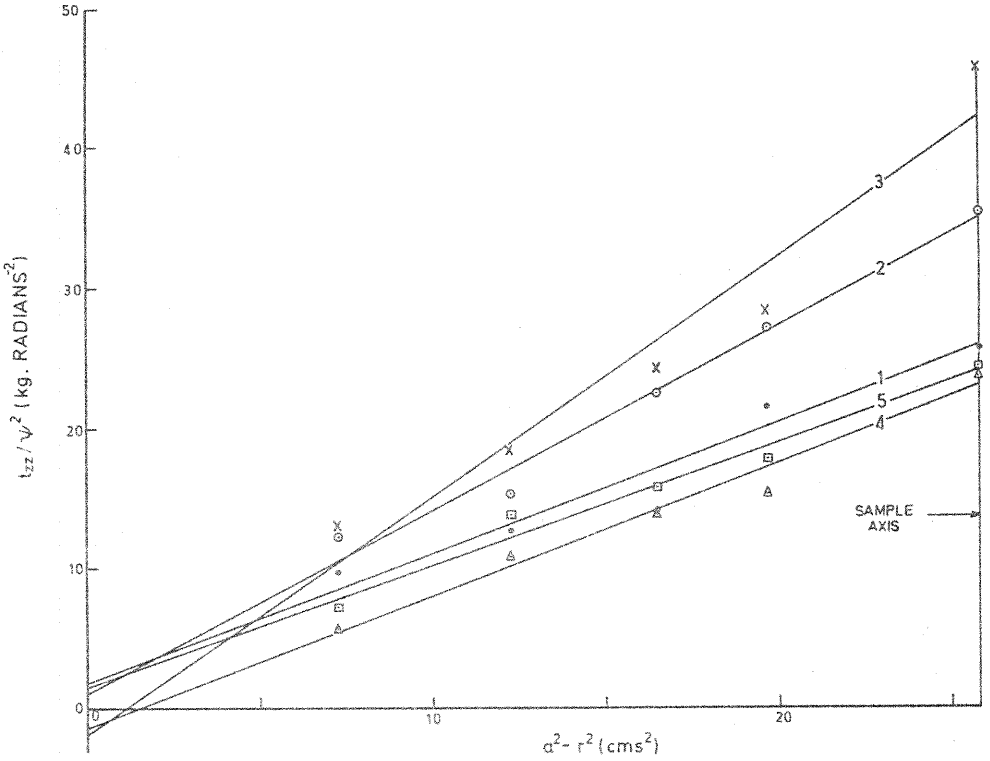

FIGURE .27. THE EXAMINATION OF EQUATION 4.9 TO FIND C_1 AND C_2 (2 MINUTE READINGS AT $\psi_a = 1.0$, ψ DECREASING).

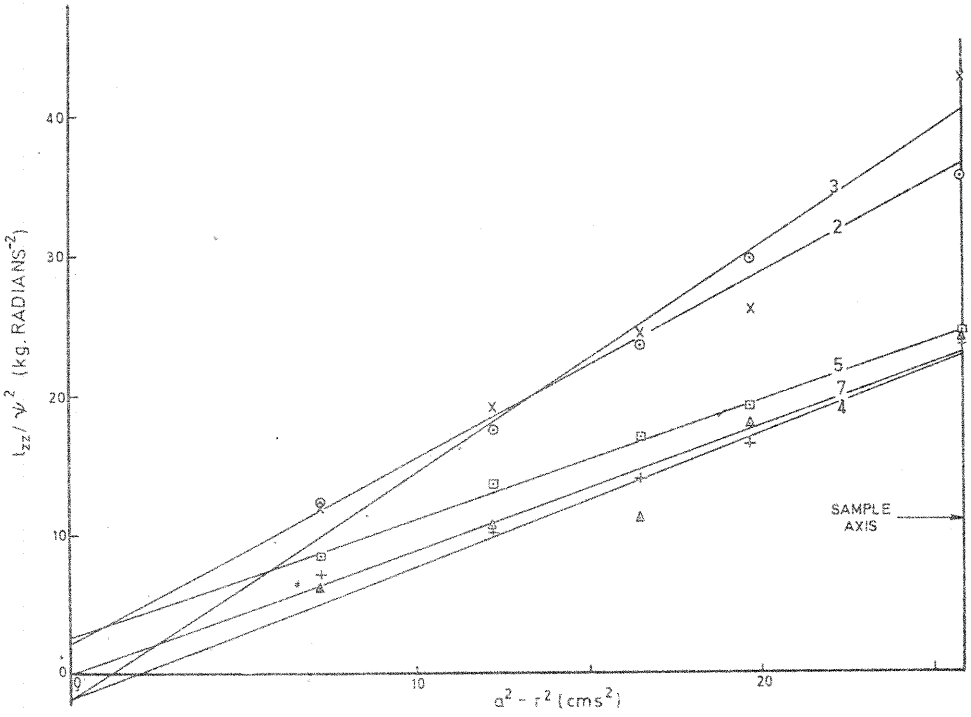

FIGURE .28. THE EXAMINATION OF EQUATION 4.9 TO FIND C_1 AND C_2 (10 MINUTE READINGS AT $\psi_a = 1.0$, ψ DECREASING).

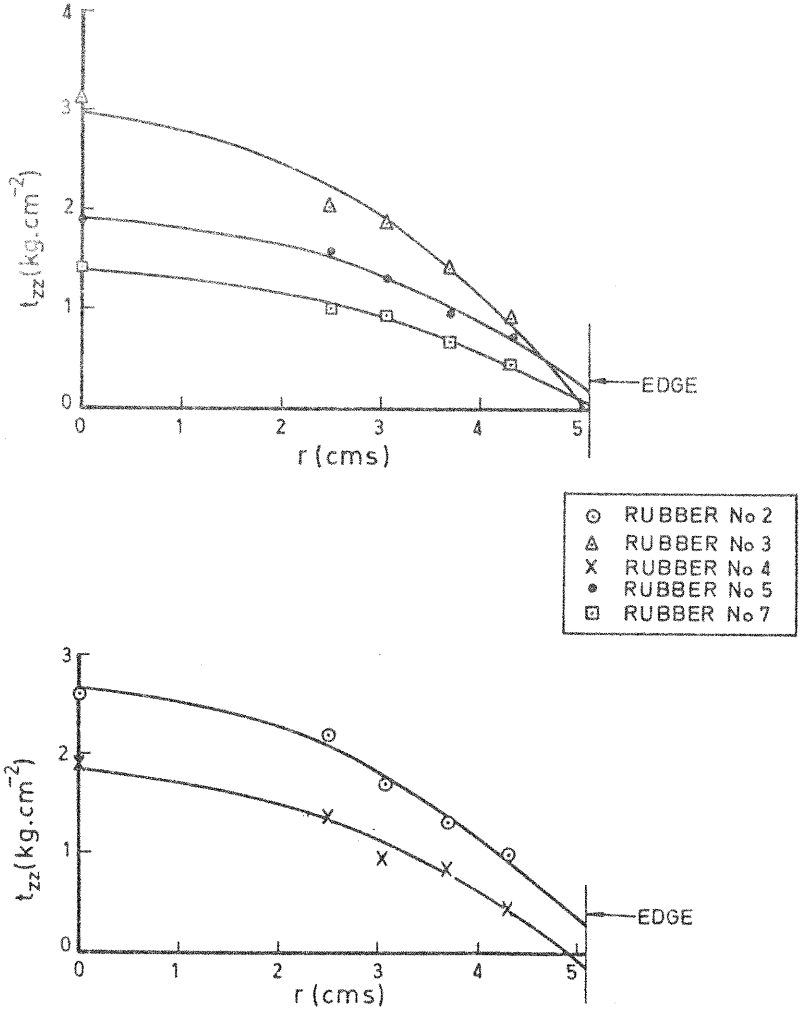

FIGURE 29 THE MOONEY NORMAL STRESS DISTRIBUTION
(10 MINUTE READINGS AT Ψ_a = 1·3, Ψ INCREASING)

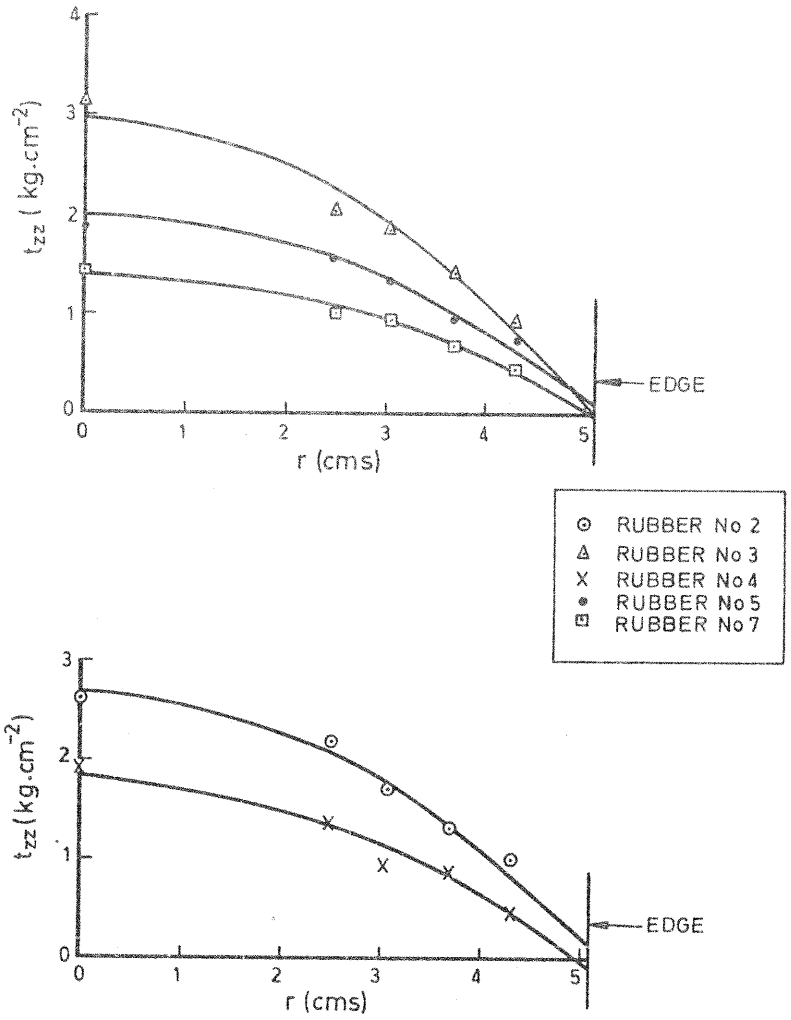

FIGURE 30 THE GENT-THOMAS NORMAL STRESS DISTRIBUTION
(10 MINUTES READINGS AT Ψ_a=1·3, Ψ INCREASING)

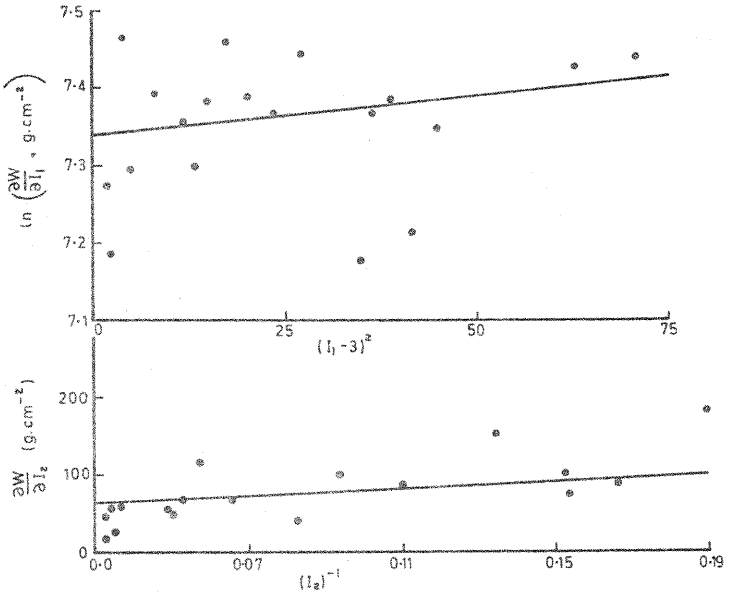

FIGURE 31 DATA FROM TABLE 7 ON RUBBER No.7

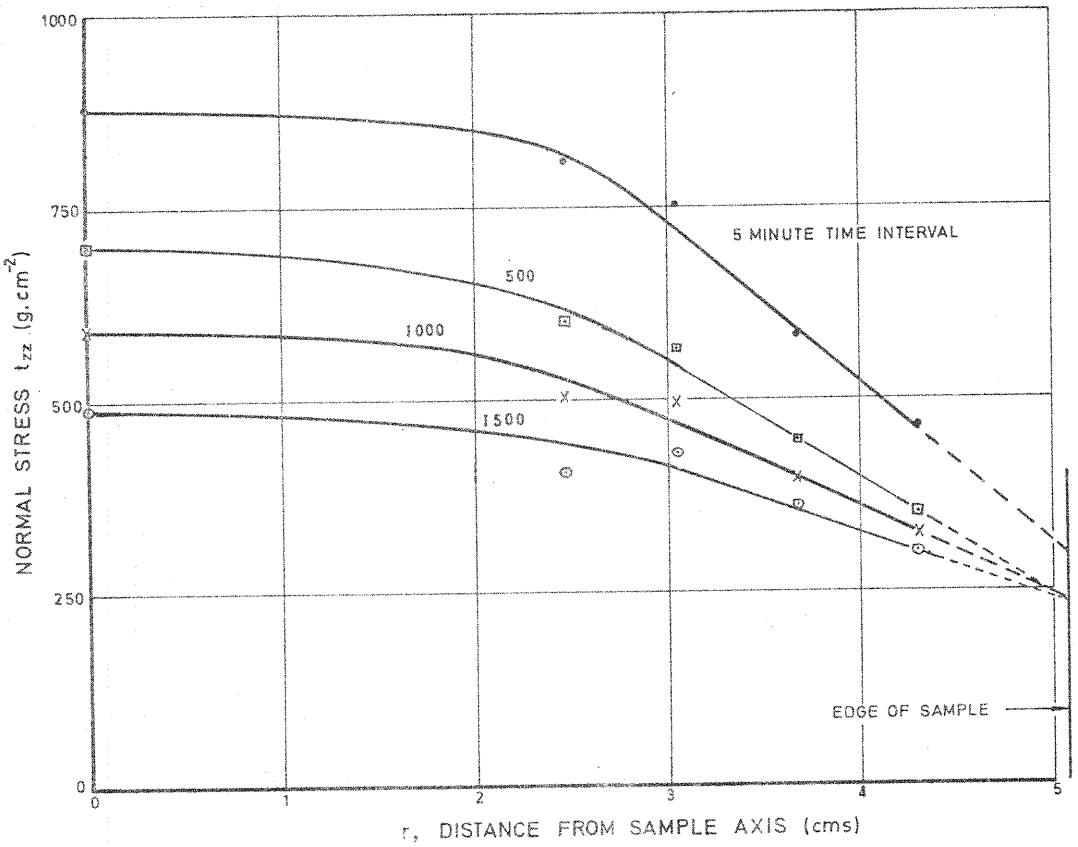

FIGURE 32. NORMAL STRESS DISTRIBUTIONS FOR RUBBER No. 6. AT 132% SURFACE SHEAR STRAIN. THE STRESSES WERE MEASURED 5, 500, 1000, AND 1500 MINUTES AFTER APPLICATION OF THE STRAIN.

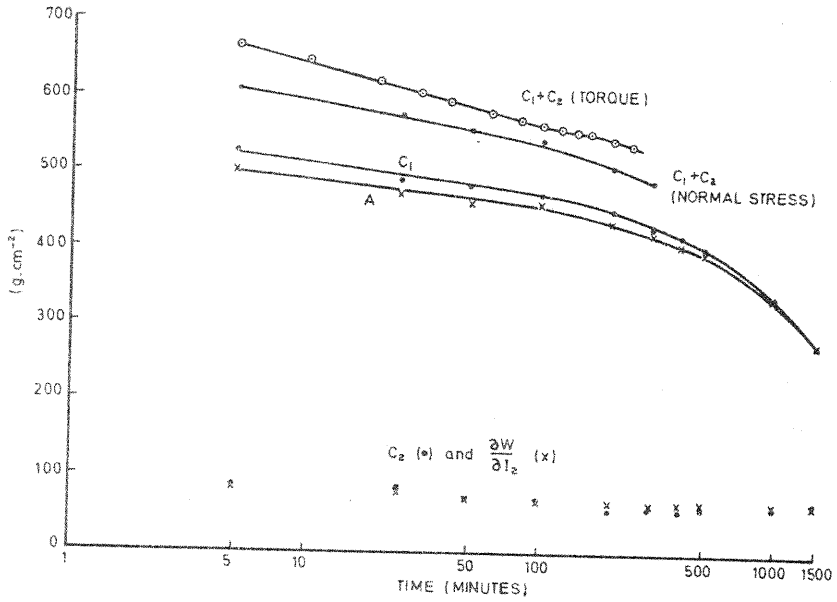

FIGURE 33 THE VARIATION OF C_1, C_2, A, AND $\frac{\partial W}{\partial I_2}$ WITH TIME FOR RUBBER No. 6. C_1+C_2 DETERMINED FROM THE NORMAL STRESSES IS COMPARED WITH C_1+C_2 FROM THE TORQUE.

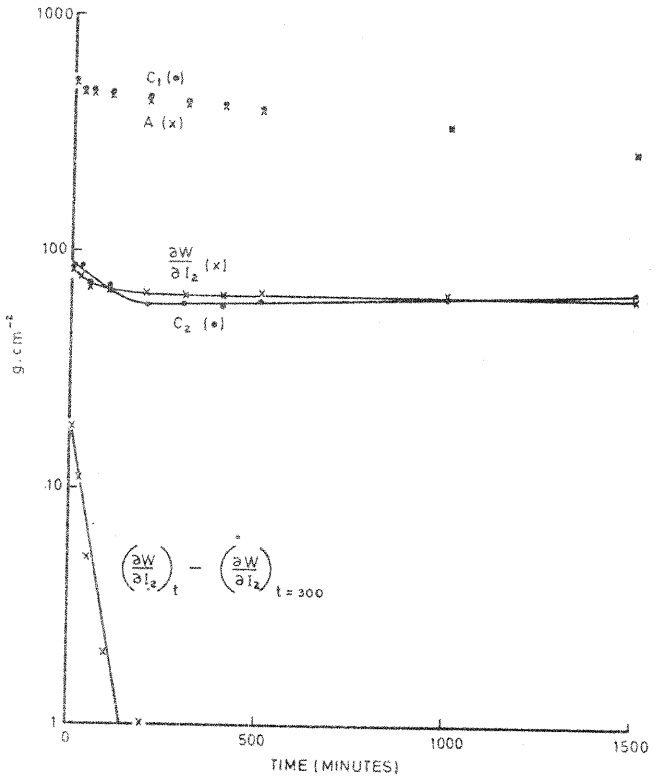

FIGURE 34 THE VARIATION OF C_1, A, C_2 AND $\frac{\partial W}{\partial I_2}$ WITH TIME FOR RUBBER No. 6.
THE DATA FOR $\frac{\partial W}{\partial I_2}$ IS REPLOTTED AS $\left(\frac{\partial W}{\partial I_2}\right)_t - \left(\frac{\partial W}{\partial I_2}\right)_{t=300}$

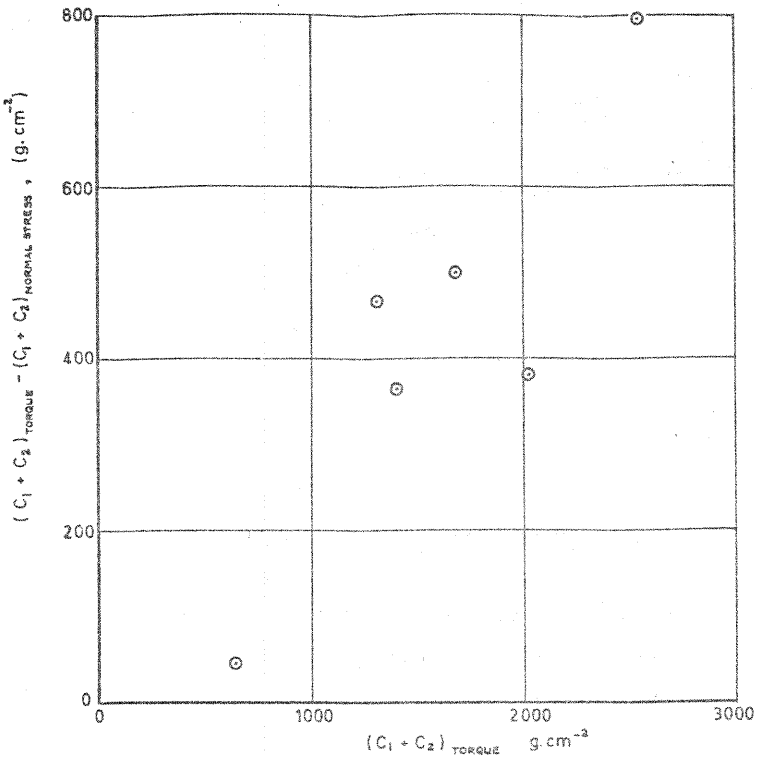

FIGURE 35 THE DIFFERENCE BETWEEN THE VALUES C_1+C_2, AS A FUNCTION OF THE RUBBER STIFFNESS. THE STIFFNESS CRITERION IS C_1+C_2 FROM THE TORQUE MEASUREMENT

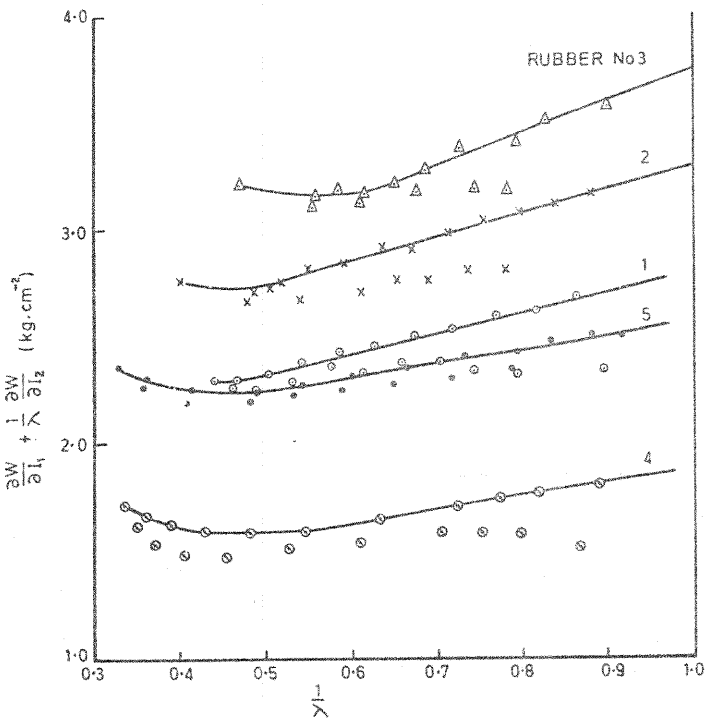

FIGURE 36. SIMPLE EXTENSION DATA FROM TABLE 17

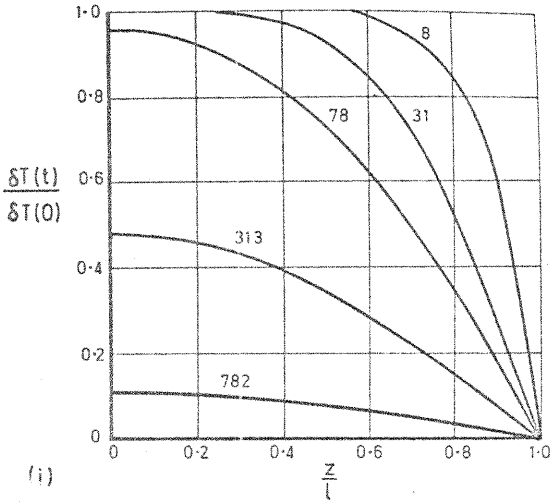

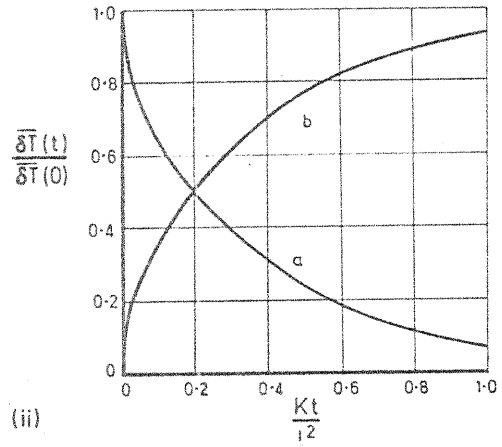

FIGURE 37

(i) THE TEMPERATURE AT Z ($-l<Z<l$) FOR CONDUCTION TIMES 8 to 782 SECONDS

(ii) THE TIME VARIATION OF THE MEAN TEMPERATURE
- (a) DUE TO CONDUCTION FROM THE SAMPLE
- (b) DUE TO AN AMBIENT TEMPERATURE INCREASE.